JCTC Journal of Chemical Theory and Computation

Article

pubs.acs.org/JCTC

The Cobalt−Methyl Bond Dissociation in Methylcobalamin: New Benchmark Analysis Based on Density Functional Theory and Completely Renormalized Coupled-Cluster Calculations

Pawel M. Kozlowski* and Manoj Kumar

Department of Chemistry, University of Louisville, 2320 South Brook St., Louisville, Kentucky 40292, United States

Piotr Piecuch,* Wei Li, Nicholas P. Bauman, and Jared A. Hansen

Department of Chemistry, Michigan State University, 578 S. Shaw Lane, East Lansing, Michigan 48824, United States

Piotr Lodowski and Maria Jaworska

Institute of Chemistry, University of Silesia, Szkolna 9, PL-40 006 Katowice, Poland

Supporting Information

ABSTRACT: The Co−C_{Me} bond dissociation in methylcobalamin (MeCbl), modeled by the Im−[Co^{III}corrin]−Me^+ system consisting of 58 atoms, is examined using the coupled-cluster (CC), density-functional theory (DFT), complete-active-space self-consistent-field (CASSCF), and CASSCF-based second-order perturbation theory (CASPT2) approaches. The multilevel variant of the local cluster-in-molecule framework, employing the completely renormalized (CR) CC method with singles, doubles, and noniterative triples, termed CR-CC(2,3), to describe higher-order electron correlation effects in the region where the Co−C_{Me} bond breaking takes place, and the canonical CC approach with singles and doubles (CCSD) to capture the remaining correlation effects, abbreviated as CR-CC(2,3)/CCSD, is used to obtain the benchmark potential energy curve characterizing the Co−C_{Me} dissociation in the MeCbl cofactor. The Co−C_{Me} bond dissociation energy (BDE) resulting from the CR-CC(2,3)/CCSD calculations for the Im−[Co^{III}corrin]−Me^+ system using the 6-31G* basis set, corrected for the zero-point energies (ZPEs) and the effect of replacing the 6-31G* basis by 6-311++G**, is about 38 kcal/mol, in excellent agreement with the experimental values characterizing MeCbl of 37 ± 3 and 36 ± 4 kcal/mol. Of all DFT functionals examined, the best dissociation energies and the most accurate description of the Co−C_{Me} bond breaking in the Im−[Co^{III}corrin]−Me^+ system are provided by B97-D and BP86 corrected for dispersion using the D3 correction of Grimme et al., which give 35 and 40 kcal/mol, respectively, when the 6-311++G** basis set is employed and when the results are corrected for ZPEs and basis set superposition error. None of the other DFT approaches examined provide results that fall into the experimental range of the Co−C_{Me} dissociation energies in MeCbl of 32−40 kcal/mol. The hybrid DFT functionals with a substantial amount of the Hartree−Fock (HF) exchange, such as B3LYP, considerably underestimate the calculated dissociation energies, with the magnitude of the error being proportional to the percentage of the HF exchange in the functional. It is argued that the overstabilization of diradical structures that emerge as the Co−C_{Me} bond is broken and, to some extent, the neglect of dispersion interactions at shorter Co−C_{Me} distances, postulated in previous studies, are the main factors that explain the substantial underestimation of the Co−C_{Me} BDE by B3LYP and other hybrid functionals. Our calculations suggest that CASSCF and CASPT2 may have difficulties with providing a reliable description of the Co−C_{Me} bond breaking in MeCbl, since using adequate active spaces is prohibitively expensive.

1. INTRODUCTION

The B_{12} cofactors, such as methylcobalamin (MeCbl) or coenzyme B_{12} [AdoCbl or (5′-deoxy-5′-adenosyl)cobalamin], are highly complex, naturally occurring organometallic compounds that contain a unique σ Co−C bond (Figure 1). MeCbl and AdoCbl serve as cofactors for a series of enzymes that catalyze complex molecular transformations.[1−19] In particular, MeCbl is the cofactor in a class of enzymes that catalyze the intermolecular methyl (Me) transfer reactions.[10,16,18] On the other hand, AdoCbl catalyzes rearrangement reactions that are mediated by radical intermediates.[2,8,9,12,13] The most remarkable aspect of the enzymatic catalysis employing coenzyme B_{12} is the observed rate enhancement, which exceeds that of the uncatalyzed reaction taking place in solution by about 12 orders of magnitude for the AdoCbl-dependent enzymes.[20,21] In all of these enzymes, the rapid cleavage of the organometallic Co−C bond constitutes one of the critical steps of their catalytic cycles. The Co−C bond is of moderate strength, and its bond dissociation energy (BDE) lies in the range of 32−40 kcal/mol for MeCbl[22,23] and 24−35 kcal/mol for AdoCbl.[24−26]

Taking into account that cleavage of the Co−C bond is not a rate-determining step,[27−30] its strength must be significantly

Received: May 4, 2011
Published: April 17, 2012

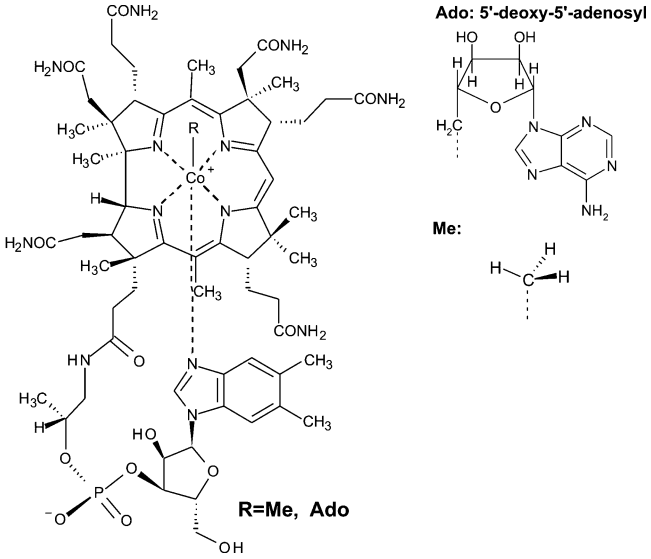

Figure 1. Molecular structure of B_{12} cofactors (R = Me or Ado).

reduced, by ∼50%, in order to achieve the observed rate enhancement.[31] However, the mechanism of the Co−C bond activation remains elusive. Because of this situation, computational modeling has become an indispensable guiding tool for understanding the mechanism of the Co−C bond activation in the B_{12} cofactors. Due to the size and complexity of the B_{12} cofactors (Figure 1), where the full structure of MeCbl has 183 atoms, with AdoCbl being even larger (209 atoms), at present density functional theory (DFT) is the most widely used computational tool to study structural and electronic properties of such bioinorganic systems. However, it should be noted that there has been a lot of activity, which dates back to the 1980s,[32−35] in the area of extending high-level *ab initio* methods, including those based on coupled-cluster (CC) theory,[36,37] to larger molecular systems through the local correlation[38−55] and fragmentation[56−60] approaches, and code parallelization.[61,62]

Several groups have started using DFT to model B_{12} cofactors. However, early applications[63−67] using the popular B3LYP functional[68,69] (which is often recommended for modeling bioinorganic complexes[70]) revealed a significant underestimation of the Co−C BDE, by ∼10−15 kcal/mol in the case of MeCbl and AdoCbl. An important step toward explaining why the hybrid B3LYP functional fails to correctly reproduce the dissociation of the Co−C bond was presented by Jensen and Ryde.[71] For MeCbl, they examined possible sources of discrepancy between experimental results and theory, including basis set, relativistic, and solvent effects and zero-point energies (ZPEs). They found out that the problem is related to the nature of the B3LYP functional, which can, in turn, be traced to the inclusion of the exact Hartree−Fock (HF) exchange, and showed that the problem is not only restricted to MeCbl but is, in general, related to homolysis of metal−carbon (M−C) bond in tetrapyrrolic systems. It was thus concluded that the more appropriate description of the M−C bond can be provided using GGA-type (generalized-gradient-approximation-type) pure functionals, such as, for example, BP86.[72] This finding was extended to other cobalamins by Kozlowski et al.,[73] who, in addition to Co−C BDEs, analyzed other properties, such as axial bond lengths. Consequently, the BP86 functional was widely applied to study structural, electronic, and spectroscopic features of B_{12} cofactors, including isolated and enzyme-bound complexes.[74−83]

It is worth mentioning that similar problems, pertaining to the difficulties the B3LYP and other hybrid density functionals face in describing the M−C bond dissociations, have also been observed in other bioinorganic-chemistry-related applications involving the formation of diradical structures (see, e.g., refs 84 and 85; note that the MeCbl and AdoCbl systems with a stretched Co−C bond are formally diradicals where the degree of diradical character is directly proportional to the Co−C distance). Methods that provide a correct description in such cases are the completely renormalized (CR) CC approaches,[86−88] including the size extensive, left-eigenstate CR-CC method with singles, doubles, and noniterative triples, abbreviated as CR-CC(2,3).[88] In general, the CR-CC(2,3) approach provides an accurate description of single bond breaking, potential energy surfaces (PESs) involving diradicals, and thermochemistry, even when using spin- and symmetry-adapted restricted HF (RHF) references (cf., e.g., refs 84 and 88−90), enabling one to achieve chemical (∼1 kcal/mol) accuracy in such situations relative to the reliable experimental or other high-level *ab initio* data, when the sufficiently large basis sets (of triple-zeta plus polarization and diffuse function quality) are employed,[89a−c,f−i] or relative to the exact, full configuration interaction (CI) or near full CI calculations in benchmark studies involving smaller basis sets,[88,89d,e] with an ease of use and at the computer effort similar to the standard, single-reference CCSD(T) approach,[91] which is accurate near the equilibrium geometries but fails in bond breaking/diradical situations. In this work, we use the multilevel variant of the local correlation extension of the CR-CC(2,3) approach,[46,47] employing a suitable generalization[48] of the cluster-in-molecule (CIM) ansatz,[45−47] which enables one to combine different CC or CC and non-CC levels of *ab initio* electronic structure theory to treat different regions in a large molecular system without splitting it into *ad hoc* fragments and saturating dangling bonds. It has been established that the local CIM-CR-CC(2,3) methodology produces high-accuracy results for single bond breaking and reaction pathways involving large systems with dozens or even hundreds of atoms, including covalent as well as noncovalent interactions,[46,48,49] reproducing the relative energetics of the corresponding canonical CR-CC(2,3) theory to within a fraction of kcal/mol at a small fraction of the computer costs. This gives us an opportunity to set the much needed high-level *ab initio* benchmark for the $Co-C_{Me}$ bond dissociation in the MeCbl system that can help to assess the accuracy of other (mainly DFT, but also CASSCF[92] and CASPT2[93]) methods.

Without benchmarks of this kind and in the absence of precise information about PESs characterizing the Co−C bond breaking in cobalamins, it is difficult to make more definitive judgments about the performance of various DFT methods that are usually the only approaches one can afford in calculations for such systems. For example, contrary to the aforementioned view regarding the performance of the GGA-type vs hybrid (e.g., B3LYP) functionals, in which a significant percentage of the HF exchange is regarded as the main source of errors, Siegbahn et al. suggested that the main source of the observed discrepancy between the experimental and B3LYP BDEs is an inadequate treatment of dispersion (i.e., van der Waals) effects by the B3LYP functional.[94,95] An exaggeration of the HF exchange in B3LYP, which the authors of refs 94 and 95 reduce

from 20 to 15% through the use of the B3LYP* functional[96] to improve the calculated BDE values, is regarded in refs 94 and 95 as a secondary problem. Taking into account that the standard formulation of DFT fails to correctly predict van der Waals interaction energies for systems with substantial dispersion interactions and seeing the significant improvements in the B3LYP and B3LYP* results reported in refs 94 and 95 which the approximate inclusion of these interactions offers, it certainly makes sense to consider dispersion forces as a possibly primary source of errors. On the other hand, considering the great variation among the DFT results for the Co−C_{Me} BDE in MeCbl with and without dispersion, reported recently in ref 97 (see, also, ref 98), which we also observe in the DFT calculations reported in this work, it is rather difficult to make definitive claims of this kind without having access to the independent high-level *ab initio* data.

The above discussion is further complicated by the fact that several DFT-based schemes have been proposed to calculate intermolecular interaction energies with significant contributions from dispersion forces (see, e.g., refs 99−104). One of them, which has gained a lot of popularity, involves the addition of the DFT dispersion energies computed from simple functions of atom−atom distances and referred to as the DFT+D methodology.[100] Although, as shown in refs 94 and 95, the approximate inclusion of dispersion via Grimme's empirical corrections to B3LYP and B3LYP* energies brings the calculated Co−C BDE values for MeCbl and AdoCbl closer to experimental values, particularly in the B3LYP*+D case, a question arises of how the dispersion interactions, which are the weaker effects that appear in the second and higher orders of the *intermolecular* perturbation theory,[105] can be responsible for the large, ∼10−15 kcal/mol or about 30%, underestimation of the Co−C BDEs in the MeCbl and AdoCbl cofactors by the B3LYP* approach (at the unmodified B3LYP level, the BDE underestimation compared to experimental results is even larger). In fact, the B3LYP+D calculations presented in refs 94 and 95 imply that the substantial underestimation of the Co−C BDEs in MeCbl and AdoCbl in the B3LYP calculations would have to originate from the equally substantial amount of energy, on the order of 11−13 kcal/mol, missing in the corresponding ground-state B3LYP or B3LYP* energies at the equilibrium geometries. This finding is not easy to understand from the point of view of the well-established interpretation of dispersion interactions as *intermolecular* correlation effects, although, as shown in ref 97, the large "+D" corrections in MeCbl observed by Siegbahn and co-workers,[94,95] which are much larger than the dispersion interaction energies of the methyl radical with typical molecular environments, may result if we account for many small interactions between methyl and cobalt and between the methyl group and atoms of other ligands of MeCbl when the short Co−C_{Me} bond is formed. The latter observation certainly helps the discussion, but even this physically appealing explanation faces challenging questions. For example, if the dispersion forces were as large at shorter distances as in the case of the B3LYP+D and B3LYP*+D calculations reported in refs 94 and 95, one would then have to argue that the previously reported BP86 results for the Co−C_{Me} BDE in MeCbl[71,73] may no longer be good once the dispersion corrections are added to them.[95] This would, however, contradict the existing numerical evidence. Indeed, as demonstrated in this work, the BP86+D results are quite reasonable once the larger basis set of the triple-zeta plus polarization quality augmented with diffuse functions is used and the effect of the basis set superposition error (BSSE) on the calculated BDE is accounted for.

To further this debate, we should also keep in mind that even if it is assumed that the covalent bond between two atoms and the associated electron density that changes upon its elongation are strongly affected by dispersion, an intuitively consistent physical picture should be produced when the nonbonded interactions (dispersion interaction between fragments) are taken into account. In particular, the corrin−Me dispersion component in MeCbl would have to be much smaller than the analogous corrin−Ado dispersion component in AdoCbl, taking into account noticeable interactions between π-orbital-containing fragments and significant differences between the sizes of the Me and Ado groups (Figure 1). However, contrary to this expectation, the dispersion-corrected B3LYP calculations of Siegbahn et al.[94,95] show that dispersion contributions in both cases are comparable, i.e., ∼11 kcal/mol in the corrin−Me case vs ∼13 kcal/mol in the case of corrin−Ado interactions. This suggests possible mixing of dispersion interactions and other many-electron correlation effects and potential conceptual difficulties with interpreting the discrepancies between the B3LYP and experimental BDEs in terms of dispersion interactions only. As shown in ref 97, there is a great deal of variation among the "+D" corrections to the Co−C_{Me} BDE in MeCbl resulting from various DFT functionals, from about 5 to 11 kcal/mol, when the "+D2" correction of ref 100b is employed, and from about 4 to 11 kcal/mol, when the more recent and more elaborate "+D3" correction of ref 100c is utilized, suggesting that dispersion interactions and other many-electron correlation effects cannot be cleanly decoupled within the DFT+D methodology and that the final calculated BDE values must eventually depend on the behavior of the underlying DFT functional at larger Co−C separations in MeCbl and similar systems. As concluded in ref 97, it is not meaningful to discuss which DFT method gives the most accurate estimate of the dispersion contributions to the calculated BDEs, in contrast to the definitive recommendations in ref 98 about the superior performance of functionals such as B3LYP*+D2. Although the added dispersion energy corrections diminish the variation among various GGA functionals, a gap persists between the results obtained with the GGA and hybrid functionals, even when both are corrected for dispersion interactions, resulting in a very wide range of BDE values that different DFT methods, with and without dispersion corrections, produce.[98]

The above discussion clearly shows that the main problem with the understanding of the issues regarding the performance of various DFT methods is the lack of independent and reliable *ab initio* data for the Co−C bond dissociation curves in the MeCbl and AdoCbl systems. In the case of the MeCbl cofactor, which is the focal point of the present work, the experimental values of the Co−C_{Me} BDEs are determined as 37 ± 3 kcal/mol (ref 22; thermolysis measurement in ethylene glycol) and 36 ± 4 kcal/mol (ref 23; photoacoustic calorimetry analysis), i.e., they have rather significant error bars. Moreover, no reliable (experimental or theoretical) information is available about the Co−C_{Me} dissociation curve. All of this complicates the discussion of the performance of various DFT approaches, as the range of Co−C BDEs resulting from experiments, including the experimental uncertainties, of 32−40 kcal/mol in the MeCbl case, is too wide for validating the use of a particular DFT-based model solely on the basis of experimental data. Moreover, without knowing the potential energy curve along

the Co−C bond breaking coordinate, one cannot even tell if the agreement between a specific DFT value of BDE and the uncertain experimental BDE values is based on the ability of a particular DFT model to capture the relevant physics. Considering the wide range of BDE values resulting from various DFT and DFT+D calculations observed in the previous studies[97] (the present study shows an even more troubling variation) and considering the fact that the DFT BDE values are strongly affected by the type of the functional, the inclusion of dispersion interactions and the specific method of including them, and, to some extent, by other factors, such as solvation effects and (also uncertain) models used to describe them, one risks the BDE calculated with a particular DFT functional and a particular treatment of dispersion and other effects becoming close to one of the experimentally available BDE values by the virtue of the fortuitous error cancellation. Because of all of these uncertainties, both in the DFT/DFT+D calculations and in the experimental BDE values, combined with the absence of robust, high-level, *ab initio* information, and contrary to the statements made in ref 98, it is not possible to unambiguously decide which functionals give the best BDE values in the MeCbl system. The results presented in ref 97 lead to a similar conclusion. To provide further insights and to aid a variety of DFT and DFT+D calculations for MeCbl, the authors of ref 97 performed auxiliary *ab initio* wave function calculations using the local correlation formulation of the second-order Møller−Plesset perturbation theory (MP2)[106] and CC theory with singles and doubles (CCSD),[107] developed in ref 40a−d, for the $Co(NH_3)_5(Me)^{2+}$ model complex[108] in its lowest-energy singlet state, but it is well established that neither MP2 nor CCSD can provide quantitative information about the BDE values in covalently bound molecular systems. They may serve as a source of qualitative information about the magnitude of dispersion interactions, which the authors of ref 97 focused on, but they cannot address the pressing issue of the lack of high-level *ab initio* data for the BDE characterizing the $Co-C_{Me}$ bond dissociation in MeCbl, which makes the more quantitative assessment of the performance of various DFT methods virtually impossible. Moreover, no attempt was made in ref 97 to prove that their local correlation MP2 and CCSD results for the $Co(NH_3)_5(Me)^{2+}$ model system are in good agreement with the corresponding canonical MP2 and CCSD calculations which can, as shown in this work, be performed at the much higher CC levels, such as CR-CC(2,3).

The present study addresses at least some of the above problems by providing, for the first time, the robust, high-level *ab initio* wave function benchmark data for the $Co-C_{Me}$ bond dissociation in MeCbl that are subsequently used to examine the performance of various DFT approaches, where all of the wave function and DFT calculations are performed in a consistent manner, using the same types of basis sets and identical nuclear geometries. Our main objective is to use the carefully validated, multilevel, variant[48] of the local correlation CIM-CR-CC(2,3) method,[46] abbreviated throughout this article as CR-CC(2,3)/CCSD, employing the robust and thoroughly benchmarked[84,88−90] completely renormalized triples corrections of the CR-CC(2,3) theory[88] to describe the chemically active region where the $Co-C_{Me}$ bond breaking takes place, the canonical CCSD approach[107] to describe the bulk of the remaining many-electron correlation effects in the chemically active and inactive regions, and the generalized single-environment CIM (GSECIM) algorithm[48] to define local orbital domains, which is well-suited to handle covalent as well as noncovalent interactions, to obtain the high-accuracy, CR-CC(2,3)-quality, benchmark potential energy curves and the corresponding BDE values characterizing the $Co-C_{Me}$ dissociation in the MeCbl cofactor, which are subsequently used to assess the accuracy of DFT and other quantum chemistry (e.g., CASSCF and CASPT2) methods. In particular, 19 different DFT functionals of pure, hybrid, and dispersion-corrected types are selected for a comprehensive examination by comparing the resulting BDE values with those obtained experimentally[22,23] and with those generated in the reasonably converged CR-CC(2,3)/CCSD calculations mixing local CR-CC(2,3) with canonical CCSD and by comparing the $Co-C_{Me}$ dissociation energy curves computed using various DFT approaches with the analogous CR-CC(2,3)-quality curve obtained with CR-CC(2,3)/CCSD. In addition to reporting the wide variety of DFT and benchmark CR-CC(2,3)-quality results, the problem of the $Co-C_{Me}$ cleavage in MeCbl is investigated using the multireference CASSCF approach followed by the second-order perturbation theory calculations (CASPT2), which are often recommended for studies involving bond breaking. As shown in this work, CASSCF and CASPT2 encounter difficulties with providing a reliable description that would be consistent with experimental results and the carefully calibrated CR-CC(2,3)/CCSD data, since using active spaces that would be appropriate is prohibitively expensive, whereas using smaller active spaces that one can afford is insufficient to obtain the desired accuracies. Along with a large number of DFT functionals and two types of the "+D" corrections applied to the most representative DFT BDE values, we examine the role of a basis set, BSSE, and ZPEs on the calculated BDE values characterizing the $Co-C_{Me}$ cleavage in MeCbl. We do not consider solvation and thermal effects, which may affect the calculated BDE values somewhat as well[97,98] and which one cannot determine as precisely as the gas-phase BDEs,[97] but this does not diminish the value of our work. On the contrary, instead of trying to reproduce rather uncertain experimental BDEs using uncertain DFT data that strongly depend on the applied functional and uncertain models of dispersion, solvation, etc., which may produce reasonable looking answers for the wrong physical reasons, we make a systematic comparison of a variety of DFT and DFT+D results with the independent, carefully executed, high-level *ab initio* CC calculations performed in exactly the same way as the DFT calculations, i.e., for the isolated MeCbl system treated with the same basis sets of increasing size. Comparisons with the experimental BDE values are made as well, but we do not base our judgments solely on comparing our DFT results with those obtained experimentally.

2. THEORY AND COMPUTATIONAL DETAILS

2.1. Structural Model. In accordance with the majority of previous computational studies, a truncated model of MeCbl was used in all calculations. The structure of the *complete* MeCbl cofactor (Figure 1), extracted from the available high-resolution X-ray crystallographic data,[109] was used as a starting point to prepare the employed structural model. All side chains of the corrin ring and the nucleotide loop were replaced by hydrogen atoms. Since the nucleotide side chain containing the negatively charged PO_4^- group has been truncated (Figure 2), the resulting structural $Im-[Co^{III}corrin]-Me^+$ model of MeCbl has a total charge of +1. The MeCbl cofactor contains dimethylbenzimidazole (DBI) as a lower axial base, but in the present calculations the DBI fragment was replaced by

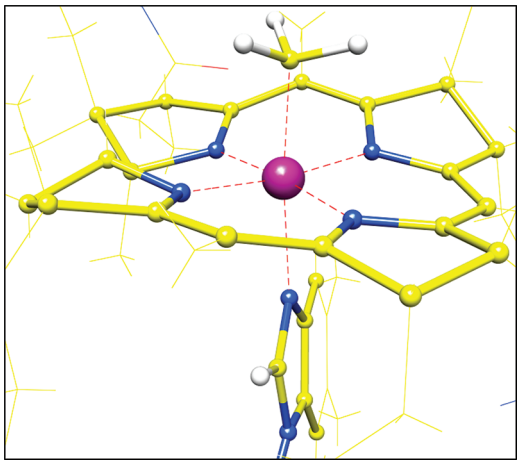

Figure 2. The structural Im−[Co^{III}corrin]−Me^{+} model of MeCbl employed in the present study (shown using ball−stick representation).

imidazole (Im). The Im−[Co^{III}corrin]−Me^{+} model has 58 atoms, instead of the 183 atoms of the full MeCbl system, making it computationally more tractable.

2.2. DFT Calculations of Nuclear Geometries, BDEs, and One-Dimensional PES Cuts for the Co−C$_{Me}$ Bond Dissociation. A variety of DFT calculations were performed using the Gaussian 03 package[110] to obtain (i) the geometries, electronic energies, and ZPEs of the Im−[Co^{III}corrin]−Me^{+} model of MeCbl and of the corresponding Im−[Co^{II}corrin]$^{+}$ and Me dissociation fragments, so that we could determine the ZPE-corrected BDE values, and (ii) the one-dimensional PES cut corresponding to the Co−C$_{Me}$ bond dissociation in Im−[Co^{III}corrin]−Me^{+}. The main geometry optimization of the Im−[Co^{III}corrin]−Me^{+} model of MeCbl shown in Figure 2, used, in particular, in the subsequent multilevel CR-CC(2,3)/CCSD, CASSCF, CASPT2, and DFT calculations for the Co−C$_{Me}$ bond dissociation, was performed using the BP86[72] approach employing the 6-31G* basis set[111] (using spherical components of the d functions). The structure of Im−[Co^{III}corrin]−Me^{+} obtained in the BP86/6-31G* calculations can be compared with the X-ray structure of Coα-(1*H*-imidazolyl)-Coβ-methylcob(III)amide.[112] The computed Co−C$_{Me}$ and Co−N$_{Im}$ bond distances of 1.969 Å and 2.130 Å, respectively, are in very good agreement with the corresponding experimental values of 1.97 and 2.09 Å.[112]

In addition to optimizing the geometry of the Im−[Co^{III}corrin]−Me^{+} model of MeCbl with the BP86/6-31G* approach, we performed a number of additional geometry optimizations using the pure, GGA-type, and hybrid functionals, including TPSS,[113] BLYP,[69,114] OLYP,[69,115] MPWPW91,[116] BHandHLYP,[117] MPW1PW91,[115,118] B3LYP,[68,69] ωB97X-D,[119] TPSSh,[120] MPW1K,[117,121] M06-2X,[122] M06,[122] B97-D,[100b] and M06-L,[123] to make comparisons with the BP86/6-31G* data. We also used all of the above functionals to determine the geometries of the Im−[Co^{II}corrin]$^{+}$ and Me radical fragments, and, after combining the purely electronic structure data with the corresponding ZPEs characterizing the equilibrium Im−[Co^{III}corrin]−Me^{+} structure and the dissociation fragments, to calculate the corresponding ZPE-corrected BDEs.

To examine the effect of a basis set on the ZPE-corrected BDE values resulting from the various DFT calculations, we used each of the above functionals to carry out the corresponding single-point computations using the larger 6-311++G** basis set[124] (with the spherical d and f functions), as implemented in Gaussian 03, at the geometries of Im−[Co^{III}corrin]−Me^{+} and the Im−[Co^{II}corrin]$^{+}$ and Me fragments optimized with the 6-31G* basis, utilizing the ZPEs determined with the 6-31G* basis set as well. Each of the resulting BDE values, obtained with the 6-31G* and 6-311++G** basis sets, was corrected for BSSE using the standard counterpoise procedure.[125] In order to examine the effect of dispersion interactions on the BDE values calculated with DFT, we exploited the "+D2" correction of ref 100b as well as the more recent and more sophisticated "+D3" correction of ref 100c, as implemented in GAMESS[126] and TURBOMOLE,[127] to correct the ZPE- and BSSE-corrected BDEs obtained with B3LYP, which serves as a representative of hybrid functionals, and BP86, representing GGA approaches, in addition to the aforementioned B97-D and ωB97X-D functionals that utilize the "+D2" correction.

To provide further insights, the BP86/6-31G*-optimized structure of Im−[Co^{III}corrin]−Me^{+} was also used to initiate the determination of the one-dimensional PES cut describing the Co−C$_{Me}$ dissociation. Thus, the Co−C$_{Me}$ bond was systematically stretched and, for a particular Co−C$_{Me}$ distance, the rest of the structure was reoptimized. It should be noted that for shorter Co−C$_{Me}$ bond distances (<2.70 Å), the restricted solution of the Kohn−Sham equations corresponds to the minimum energy, whereas at longer distances (>2.70 Å), the unrestricted solution was found to be the lowest. As shown in Figure 3, the diradical character of the Im−[Co^{III}corrin]−Me^{+} complex starts developing as the Co−C$_{Me}$ bond is stretched beyond 2.70 Å, becoming fully fledged at the Co−C$_{Me}$ distance of ∼4.0 Å. At that point, the Co ion and C$_{Me}$ have electronic spins of almost +1 and −1, respectively, implying the complete breakage of the Co−C$_{Me}$ bond. As the Co−C$_{Me}$ bond is stretched beyond 4.0 Å, the well-behaved dissociation curves become flat, and no significant changes are observed in the energy of the system. Once the one-dimensional PES cut for the Co−C$_{Me}$ bond breaking in the Im−[Co^{III}corrin]−Me^{+} system resulting from the above unrestricted BP86/6-31G* calculations was determined, we performed a series of single-point energy calculations, using a few representative DFT approaches, including hybrid (B3LYP), pure GGA (TPSS, MPWPW91, M06-L, BP86), and dispersion-corrected GGA (BP86+D2, BP86+D3, B97-D) and hybrid (B3LYP+D2, B3LYP+D3) functionals, a number of local correlation CIM-CC methods with up to triple excitations employing the RHF reference, described in section 2.3, along with the canonical, RHF-based, MP2 and CCSD computations, and the CASSCF and CASPT2 schemes, at the points along the BP86/6-31G* PES cut corresponding to the Co−C$_{Me}$ distances of 1.969 (equilibrium), 2.0, 2.4, 2.8, 3.2, 3.6, 4.0, and 4.5 Å, to obtain a variety of dissociation curves for comparison purposes (in the case of CASSCF and CASPT2, which display a different behavior at larger Co−C$_{Me}$ separations, additional geometries were added; see section 2.4). Combining DFT to obtain the geometries defining reaction pathways with the more expensive higher-level methods, such as those based on CC theory, to improve, at least potentially, the resulting energetics is a standard practice. There are a few other reasons why in calculating the various DFT and *ab initio* dissociation curves reported in this work we used the geometries along the Co−C$_{Me}$ bond breaking pathway determined in the BP86/6-31G* calculations. It is, for example, well-documented that the BP86/

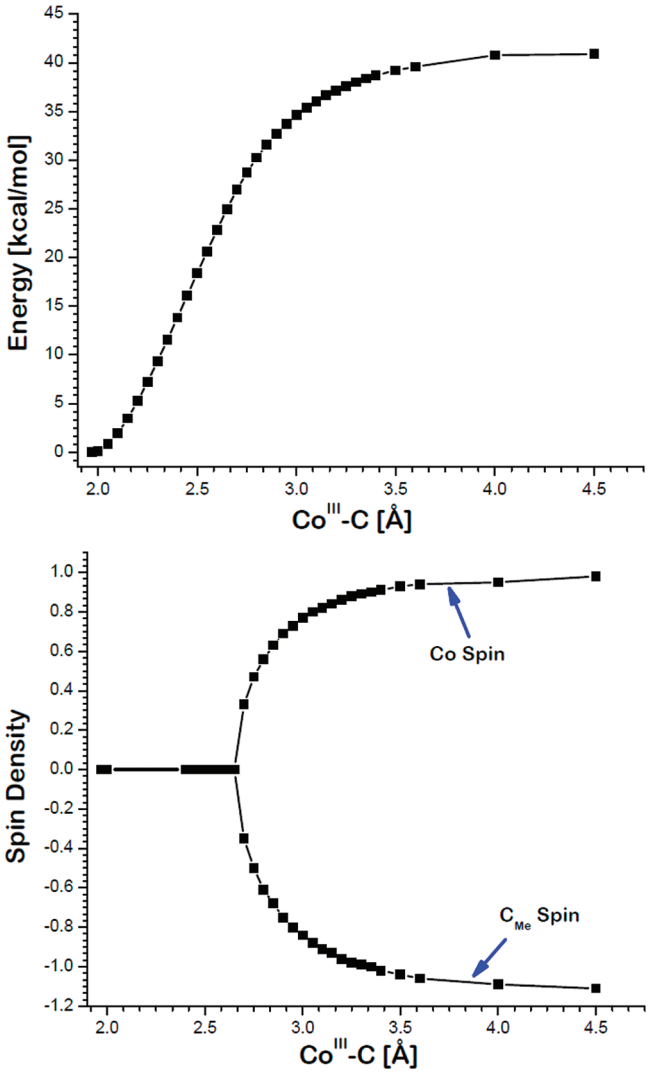

Figure 3. The BP86/6-31G*-computed dissociation curve for Im−[Co^{III}corrin]−Me$^+$ (top panel) and spin density profiles for the Co^{III} ion and the C atom of the methyl group, designated as C$_{Me}$, as a function of the Co−C$_{Me}$ bond distance (bottom panel).

6-31G* level of theory provides a reliable description of the Im−[Co^{III}corrin]−Me$^+$ geometry (cf., e.g., refs 74a and 81); our BP86/6-31G* calculations confirm this. It is also well-known that the geometries of the cobalt-containing corrinoids are almost insensitive to the change of a DFT functional[82] (cf., also section 3.2). Finally, all of the DFT, CC, and CASSCF/CASPT2 calculations of the Co−C$_{Me}$ dissociation curve of Im−[Co^{III}corrin]−Me$^+$ were carried out using the same set of geometries, all resulting from the BP86/6-31G* geometry optimizations at various Co−C$_{Me}$ bond lengths, allowing for meaningful comparisons of the dissociation curves obtained with different methods.

Since our highest-level CR-CC(2,3)/CCSD calculations, which mix local CR-CC(2,3), as applied to the chemically active region where the Co−C$_{Me}$ bond breaking takes place, with canonical CCSD to describe the remaining correlation effects in the Im−[Co^{III}corrin]−Me$^+$ system, could only be performed for the smaller 6-31G* basis set, we used the auxiliary canonical CR-CC(2,3)/6-31G* and CR-CC(2,3)/6-311++G** calculations for the related Co(NH$_3$)$_5$(Me)$^{2+}$ model complex in its lowest-energy singlet state,[108] also exploited in ref 97, to estimate the CR-CC(2,3)/CCSD/6-311++G** result for the Co−C$_{Me}$ BDE in Im−[Co^{III}corrin]−Me$^+$, which we could not obtain in a direct calculation. In order to do this, we first optimized the geometry of the Co(NH$_3$)$_5$(Me)$^{2+}$ complex using the restricted BP86 functional and the 6-31G* basis set. Then, as in the case of the Im−[Co^{III}corrin]−Me$^+$ system, we kept stretching the Co−C$_{Me}$ bond while reoptimizing the rest of the Co(NH$_3$)$_5$(Me)$^{2+}$ molecule at the restricted BP86/6-31G* level to generate the one-dimensional PES cut describing the Co−C$_{Me}$ dissociation in Co(NH$_3$)$_5$(Me)$^{2+}$ in its lowest-energy singlet state. Note that the lowest-energy Co−C$_{Me}$ dissociation channel in Co(NH$_3$)$_5$(Me)$^{2+}$ is a triplet, but we are interested in modeling the Co−C$_{Me}$ bond breaking in the Im−[Co^{III}corrin]−Me$^+$ system, which proceeds on the singlet PES, so, in analogy to the calculations reported in ref 97, we focused on the lowest-energy singlet PES of Co(NH$_3$)$_5$(Me)$^{2+}$. Once the one-dimensional cut of the lowest-energy singlet PES corresponding to the Co−C$_{Me}$ dissociation in the Co(NH$_3$)$_5$(Me)$^{2+}$ complex was generated, we performed a series of single-point canonical, RHF-based, CR-CC(2,3) calculations at the Co−C$_{Me}$ distances of 1.9575 (equilibrium), 2.2, 2.4, 2.6, 2.8, 3.0, 3.5, 4.0, and 4.5 Å using the 6-31G* and 6-311++G** basis sets. In analogy to the Im−[Co^{III}corrin]−Me$^+$ system, as the Co−C$_{Me}$ bond is stretched beyond 4.0 Å, the dissociation energy curves characterizing the Co(NH$_3$)$_5$(Me)$^{2+}$ complex become flat, and the corresponding CR-CC(2,3)/6-31G* and CR-CC(2,3)/6-311++G** energies no longer change in a substantial manner (changes are on the order of a fraction of a kcal/mol), so it is sufficient to use the Co−C$_{Me}$ distance of 4.5 Å and its equilibrium value (1.9575 Å) to obtain a reasonable estimate of the basis set effect on the Co−C$_{Me}$ BDE resulting from the CR-CC(2,3)-level calculations. Moreover, as shown in section 3.1, the differences between the CR-CC(2,3)/6-311++G** and CR-CC(2,3)/6-31G* energies at larger Co−C$_{Me}$ separations in the Co(NH$_3$)$_5$(Me)$^{2+}$ complex are almost (to within a fraction of a kcal/mol) constant when the Co−C$_{Me}$ distance becomes larger than 3.5 Å. Thus, the final CR-CC(2,3)/CCSD/6-311++G** result for the BDE characterizing the Co−C$_{Me}$ bond dissociation in the Im−[Co^{III}corrin]−Me$^+$ system was estimated by adding the difference between the BDEs obtained in the canonical CR-CC(2,3)/6-311++G** and CR-CC(2,3)/6-31G* calculations for the Co(NH$_3$)$_5$(Me)$^{2+}$ model complex to the ZPE-corrected BDE obtained in the multilevel CR-CC(2,3)/CCSD calculations for the Im−[Co^{III}corrin]−Me$^+$ molecule using the 6-31G* basis set. Each electronic dissociation energy needed to estimate the CR-CC(2,3)/CCSD/6-311++G** BDE value for the Im−[Co^{III}corrin]−Me$^+$ molecule, as explained above, was calculated using the formula $E(R_{Co-C} = 4.5\ Å) - E(R_{Co-C,e})$, where $R_{Co-C,e}$ is the appropriate equilibrium geometry obtained in the relevant BP86/6-31G* optimization, and $R_{Co-C} = 4.5$ Å is the geometry resulting from the corresponding BP86/6-31G*-level partial optimization in which the Co−C$_{Me}$ distance is fixed at 4.5 Å.

2.3. CC Calculations. A variety of CC calculations employing the same 6-31G* (Im−[Co^{III}corrin]−Me$^+$ and Co(NH$_3$)$_5$(Me)$^{2+}$) and 6-311++G** [Co(NH$_3$)$_5$(Me)$^{2+}$] basis sets as those used in the DFT calculations, with the main focus on the carefully validated CR-CC(2,3)/CCSD methodology, were performed to establish the benchmark potential energy curve for the Co−C$_{Me}$ bond breaking in the Im−[Co^{III}corrin]−Me$^+$ model of MeCbl and the benchmark BDE value. Let us recall that the CR-CC(2,3) approach, in

which one adds a suitably designed noniterative correction due to connected triple excitations to the CCSD energy,[88] represents a rigorously size-extensive CC method which provides a highly accurate description of single bond breaking, diradicals (including transition metal systems), and covalent as well as noncovalent interactions with an effort similar to conventional CCSD(T) calculations. The "only" problem with the canonical CR-CC(2,3) approach exploiting the delocalized HF orbitals (RHF orbitals throughout this work) is that the CPU time of the CR-CC(2,3) calculation scales as N^6 in the CCSD part and N^7 in the triples correction part with the system size N, with memory requirements scaling as N^4, making the canonical CR-CC(2,3) calculations for systems of the Im−[Co^{III}corrin]−Me$^+$ size prohibitively expensive. The CR-CC(2,3)/CCSD methodology enabled us to address this issue by combining the canonical CCSD calculations for the entire Im−[Co^{III}corrin]−Me$^+$ system, which we could run in parallel using a highly scalable implementation[62] of the spin-free RHF-based CCSD algorithm for singlet ground states incorporated in the GAMESS package,[128] with the local CR-CC(2,3) treatment of the chemically active region where the Co−C$_{Me}$ dissociation takes place (see the analysis in section 3.1). The CPU timing associated with determining the triples correction of CR-CC(2,3) within the multilevel CR-CC(2,3)/CCSD computation for the Im−[Co^{III}corrin]−Me$^+$ system employing the 6-31G* basis set, run on a single core using our local correlation programs based on the CIM formalism[46−48] and interfaced with GAMESS, was only about 60 h per point on the PES, when the tightest value of the environment orbital selection threshold described below was employed. The wall time needed to complete the corresponding canonical CCSD/6-31G* calculations required (depending on the number of iterations that varied between ∼30 near the equilibrium geometry and ∼70 at larger Co−C$_{Me}$ distances, assuming the convergence threshold of 10^{-6} hartree) about 40−90 h per point on the PES when 28 cores were employed. To estimate the effect of the basis set on the Co−C$_{Me}$ dissociation energy in the Im−[Co^{III}corrin]−Me$^+$ system resulting from the CR-CC(2,3)/CCSD/6-31G* calculations, we performed the canonical CR-CC(2,3)/6-31G* and CR-CC(2,3)/6-311++G** calculations for the related Co(NH$_3$)$_5$(Me)$^{2+}$ complex in its lowest singlet state, as described in section 2.2. All of this combined enabled us to obtain the CR-CC(2,3)/6-311++G**-quality value of the Co−C$_{Me}$ BDE characterizing the Im−[Co^{III}corrin]−Me$^+$ species without running the CR-CC(2,3)/CCSD/6-311++G** or canonical CR-CC(2,3) calculations for this system.

The CR-CC(2,3)/CCSD approach belongs to a new generation of the multilevel CIM schemes, inspired by ref 48, which combine affordable lower-level canonical (rather than local[48]) *ab initio* methods to describe the bulk of the many-electron correlation effects in the entire system, including active and inactive regions, with the higher-level local schemes to describe the remaining electron correlation effects in the active region(s), without splitting the system into *ad hoc* fragments and saturating dangling bonds exploited in the ONIOM-type schemes.[129] In the case of CR-CC(2,3)/CCSD, one uses canonical CCSD to describe the entire system, including active and inactive regions, and the triples corrections of local CR-CC(2,3) to improve the description of the active region(s), where strongly correlated processes, such as bond breaking (in our case, the Co−C$_{Me}$ bond breaking in Im−[Co^{III}corrin]−Me$^+$), which CCSD does not describe in a sufficiently accurate manner, take place. To ensure that the CR-CC(2,3)/CCSD results are robust enough to serve as benchmark data, we also performed the auxiliary CCSD/MP2 and CR-CC(2,3)/MP2 calculations that combine local CCSD or local CR-CC(2,3) to treat the post-MP2 correlation effects in the active region(s) with canonical MP2 to describe the entire system. A comparison of the electronic energies along the Co−C$_{Me}$ bond breaking coordinate resulting from the CCSD/MP2 and canonical CCSD calculations enabled us to validate the appropriateness of our CIM orbital subsystem, which represents the active region of the Im−[Co^{III}corrin]−Me$^+$ molecule where the Co−C$_{Me}$ bond dissociation occurs, depicted in Figure 4, and the correctness of our final choice

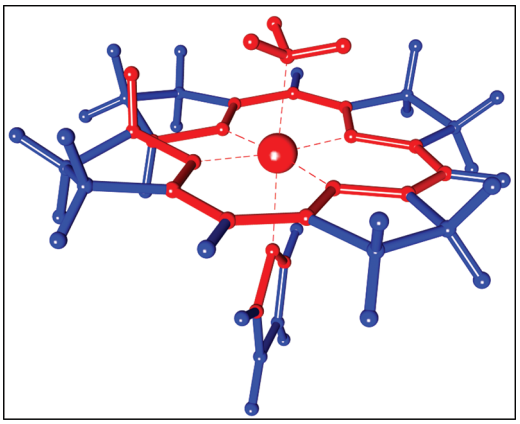

Figure 4. The structural Im−[Co^{III}corrin]−Me$^+$ model of MeCbl used in this work, with the red-colored zone marking the atoms that can be assigned to the CIM subsystem, which in the multilevel X/Y calculations using the 6-31G* basis set is treated by the higher-level method X. The following pairs (X,Y) of higher-level local (X) and lower-level canonical (Y) methods are considered in the present study: (CR-CC(2,3),CCSD), which is the main result, (CR-CC(2,3),MP2), and (CCSD,MP2) (see the main text for details).

of the CIM parameter ζ, which was used to define this subsystem through a suitable analysis of the occupied localized molecular orbitals (LMOs; see the additional remarks below). It also allowed us to demonstrate that by describing the bulk of the correlation energy in the active and inactive regions at the canonical MP2 level and by employing local CC to capture higher-order correlation effects in the active region neglected in MP2, one obtains an accurate representation of the corresponding canonical CC potential energy curve for the Co−C$_{Me}$ bond dissociation in Im−[Co^{III}corrin]−Me$^+$. A comparison of the analogous CR-CC(2,3)/CCSD and CR-CC(2,3)/MP2 data, which are, as shown in section 3.1, very similar, allowed us to show that the Co−C$_{Me}$ dissociation curve obtained in the CR-CC(2,3)/CCSD calculations can be regarded as converged to within ∼1 kcal/mol compared to the canonical CR-CC(2,3) results in the same basis set.

We now explain the key elements of the CCSD/MP2, CR-CC(2,3)/MP2, and CR-CC(2,3)/CCSD approaches relevant to this work. The basic idea of all CIM-CC and CIM-MPn methods[45−48] is the observation that the total correlation energy of a large system or its component, such as the triples correction of CCSD(T) or CR-CC(2,3), can be obtained as a sum of contributions from the occupied orthonormal LMOs and their respective occupied and unoccupied orbital domains that define the CIM subsystems. If the occupied LMOs,

obtained as in refs 46−49 with the Boys localization,[130] are designated by i', the CIM-CC and CIM-MPn correlation energies are calculated as[46−48]

$$\Delta E = \sum_{i'} \delta E_{i'},\ \delta E_{i'} = (1/M_{i'}) \sum_{\{P_{i'}\}} \delta E_{i'}(\{P_{i'}\}) \tag{1}$$

where $\{P_{i'}\}$ represents any orbital subsystem $\{P\}$ that contains the specific occupied LMO $\phi_{i'}$ as the so-called central orbital, and $M_{i'}$ designates the number of subsystems $\{P\}$ that contain $\phi_{i'}$ as a central orbital. The only difference between various CIM-CC and CIM-MPn approaches and their multilevel variants lies in the definitions of the $\delta E_{i'}(\{P_{i'}\})$ contributions in eq 1; we refer the reader to refs 46−48 for the expressions relevant to the CIM-MP2, CIM-CCSD, and CIM-CR-CC(2,3) calculations in the pure or multilevel form [cf., e.g., eqs 2−4 in ref 48]. In the following discussion, we designate the $\delta E_{i'}$ contributions to the correlation energy ΔE corresponding to the MP2, CCSD, and CR-CC(2,3) approaches as $\delta E_{i'}^{(\mathrm{MP2})}$, $\delta E_{i'}^{(\mathrm{CCSD})}$, and $\delta E_{i'}^{(\mathrm{CR\text{-}CC(2,3)})}$, respectively. All CIM approaches result in straightforward algorithms in which, beginning with the AO → MO integral transformation and ending up with the final CC or MPn work, the CC or MPn calculation for a large system is split into independent and relatively inexpensive calculations for CIM orbital subsystems, which are subsequently used to evaluate the correlation energy for the entire system out of the correlation energy contributions $\delta E_{i'}(\{P_{i'}\})$ extracted from the calculations for the individual CIM subsystems $\{P_{i'}\}$. In this study, we adopt the GSECIM algorithm for designing CIM orbital subsystems introduced in ref 47. The main characteristics of this algorithm are the assignment of the central occupied LMOs, which initiate the process of determining the orbital composition of each CIM subsystem, to user-specified groups of atoms in a molecule of interest with the help of the Mulliken charges and the use of a single parameter ζ to identify additional environment LMOs that are associated with the central LMOs of each CIM subsystem.

The multilevel CCSD/MP2, CR-CC(2,3)/MP2, and CR-CC(2,3)/CCSD approaches exploited in this work can be regarded as the improved variants of the previously formulated[48] GSECIM-CCSD/MP2, GSECIM-CR-CC(2,3)/MP2, and GSECIM-CR-CC(2,3)/CCSD methods, in which the local MP2 [GSECIM-CCSD/MP2, GSECIM-CR-CC(2,3)/MP2] or local CCSD [GSECIM-CR-CC(2,3)/CCSD] treatment of the CIM subsystems associated with the inactive regions is replaced by the canonical MP2 or CCSD calculations for the entire system, limiting the use of local methodology to the higher-order, post-MP2 or post-CCSD, correlation effects associated with the active region(s). To provide the formal basis for the CCSD/MP2, CR-CC(2,3)/MP2, and CR-CC(2,3)/CCSD approaches that mix the lower-level canonical and higher-level local calculations, we recall that one always initiates a given multilevel CIM calculation by labeling each nonhydrogen atom in a molecular system of interest (in the GSECIM algorithm used in this work, a group of atoms) by the *ab initio* method we want to apply to it. As explained in ref 48, the labeling of atoms by the *ab initio* methods we want to use for them translates in the multilevel CIM framework into the labeling of the occupied LMOs assigned to these atoms in the initial stages of the CIM subsystem design. Once this is done, each orbital subsystem is labeled by the quantum chemistry approach we want to apply to it. For example, if we want to treat some part of a molecule by CR-CC(2,3) and the rest of it by MP2, as in the GSECIM-CR-CC(2,3)/MP2 approach of ref 48, a CIM subsystem containing at least one occupied central LMO which is completely assigned to one or more atoms marked as the CR-CC(2,3) atom(s) is treated by CR-CC(2,3), whereas a subsystem that does not contain central LMOs that are completely assigned to the CR-CC(2,3) atoms is treated by MP2. After performing such an analysis and the CR-CC(2,3) and MP2 subsystem calculations, we determine the $\delta E_{i'}^{(\mathrm{CR\text{-}CC(2,3)})}$ contributions for the occupied LMOs i' that are central in the subsystems treated by CR-CC(2,3) and the $\delta E_{i'}^{(\mathrm{MP2})}$ contributions for the occupied LMOs i' that are central in the subsystems treated by MP2 and calculate the total correlation energy as in eq 1 to obtain

$$\begin{aligned}\Delta E &= \sum_{i'} \delta E_{i'} \\ &= \sum_{i' \in \{P_{\mathrm{CR\text{-}CC(2,3)}}\}} \delta E_{i'}^{(\mathrm{CR\text{-}CC(2,3)})} + \sum_{i' \notin \{P_{\mathrm{CR\text{-}CC(2,3)}}\}} \delta E_{i'}^{(\mathrm{MP2})}\end{aligned} \tag{2}$$

where $\{P_{\mathrm{CR\text{-}CC(2,3)}}\}$ designates subsystems treated by CR-CC(2,3). This is what we would do in the purely local GSECIM-CR-CC(2,3)/MP2 calculations [for LMOs i' being simultaneously central in the CR-CC(2,3) and MP2 subsystems, we would also perform the appropriate energy averaging to avoid overcounting, as in eq 1; see ref 48 for further information]. The CR-CC(2,3)/MP2 scheme used in this work emerges from the above considerations by performing the following manipulations in eq 2:

$$\begin{aligned}\Delta E &= \sum_{i' \in \{P_{\mathrm{CR\text{-}CC(2,3)}}\}} (\delta E_{i'}^{(\mathrm{CR\text{-}CC(2,3)})} - \delta E_{i'}^{(\mathrm{MP2})}) \\ &\quad + \sum_{i' \in \{P_{\mathrm{CR\text{-}CC(2,3)}}\}} \delta E_{i'}^{(\mathrm{MP2})} + \sum_{i' \notin \{P_{\mathrm{CR\text{-}CC(2,3)}}\}} \delta E_{i'}^{(\mathrm{MP2})} \\ &= \sum_{i' \in \{P_{\mathrm{CR\text{-}CC(2,3)}}\}} (\delta E_{i'}^{(\mathrm{CR\text{-}CC(2,3)})} - \delta E_{i'}^{(\mathrm{MP2})}) + \Delta E^{(\mathrm{MP2})} \\ &\equiv \Delta E^{\mathrm{CR\text{-}CC(2,3)/MP2}}\end{aligned} \tag{3}$$

where $\Delta E^{(\mathrm{MP2})}$ represents the canonical MP2 correlation energy for the entire system, which replaces the individual MP2 subsystem contributions in the inactive and active regions. As we can see, the CR-CC(2,3)/MP2 approach requires the determination of the post-MP2 contributions to the correlation energy captured by the CR-CC(2,3) calculations in the CIM subsystems containing central occupied LMOs that are completely assigned to the CR-CC(2,3) atoms, which are subsequently added to the canonical MP2 energy obtained for the whole system. The CCSD/MP2 and CR-CC(2,3)/CCSD methods are defined in a similar manner. Thus, we calculate the CCSD/MP2 and CR-CC(2,3)/CCSD correlation energies as

$$\Delta E^{\mathrm{CCSD/MP2}} = \sum_{i' \in \{P_{\mathrm{CCSD}}\}} (\delta E_{i'}^{(\mathrm{CCSD})} - \delta E_{i'}^{(\mathrm{MP2})}) + \Delta E^{(\mathrm{MP2})} \tag{4}$$

and

$$\begin{aligned}&\Delta E^{\mathrm{CR\text{-}CC(2,3)/CCSD}} \\ &= \sum_{i' \in \{P_{\mathrm{CR\text{-}CC(2,3)}}\}} (\delta E_{i'}^{(\mathrm{CR\text{-}CC(2,3)})} - \delta E_{i'}^{(\mathrm{CCSD})}) + \Delta E^{(\mathrm{CCSD})}\end{aligned} \tag{5}$$

respectively, where $\{P_{CCSD}\}$ and $\{P_{CR\text{-}CC(2,3)}\}$ designate the CIM subsystems treated by CCSD and CR-CC(2,3), respectively, and $\Delta E^{(CCSD)}$ is the canonical CCSD energy. It should be pointed out that in analogy to the CCSD- and CR-CC(2,3)-level calculations performed in this work, which utilized the spin-adapted, RHF-based, formulation of the CC theory, which is a typical way of using the CR-CC(2,3) approach in practice [the unrestricted CR-CC(2,3) codes do not exist], the canonical MP2 calculations needed to determine the MP2 correlation energy that enters the CCSD/MP2 and CR-CC(2,3)/MP2 energy expressions, eqs 3 and 4, respectively, were the restricted, RHF-based, MP2 calculations. We are not interested in examining the performance of the MP2 approach *per se* but, rather, in using MP2 as a way to capture the fraction of the correlation effects within the RHF-based multilevel CIM-CC framework. For this reason, we use restricted MP2 in all of our considerations, not its unrestricted analog. The same applies to the CCSD calculations needed to determine the canonical CCSD energy in eq 5.

In order to establish the desired benchmark potential energy curve for the Co−C_{Me} bond breaking in the Im−[Co^{III}corrin]−Me^+ system and the resulting BDE values, we performed a series of the increasingly accurate multilevel CC calculations, using the CCSD/MP2, CR-CC(2,3)/MP2, and CR-CC(2,3)/CCSD sequence described above and the 6-31G* basis set, at the selected points along the BP86/6-31G* PES cut listed in section 2.2. To initiate the GSECIM orbital analysis, which led to the construction of the final CIM subsystem that represents the active region of the Im−[Co^{III}corrin]−Me^+ model of MeCbl where the Co−C_{Me} bond dissociation occurs, depicted in Figure 4, we marked the Co atom and the C atom of the methyl group being dissociated out as the non-hydrogen atoms that must be treated by the higher-level *ab initio* method X of a given multilevel X/Y approach [CCSD in the CCSD/MP2 case and CR-CC(2,3) in the CR-CC(2,3)/MP2 and CR-CC(2,3)/CCSD cases]. As in all multilevel calculations based on the GSECIM algorithm, the central occupied LMOs that were assigned to these two non-hydrogen atoms and to the hydrogen atoms of the methyl group by examining the corresponding Mulliken charges (cf. refs 47 and 48 for the details) as well as the additional environment LMOs that were assigned to these central LMOs by comparing the appropriate off-diagonal elements of the Fock matrix with the threshold ζ were automatically labeled as the LMOs defining the CIM subsystem that must be treated by the higher-level theory X of the X/Y approach. After the subsequent analysis of the remaining LMOs, including the removal of redundant small domains,[47,48] and after determining the corresponding unoccupied orbitals,[46] we ended up with a final single CIM subsystem representing the active region, which in the multilevel X/Y calculations reported in this work was treated by the higher-level method X and which contained the central and environment orbitals that, after back-assigning to atoms via the Mulliken charges, produced the red-colored zone shown in Figure 4. In the highest-level CR-CC(2,3)/CCSD calculations for the Im−[Co^{III}corrin]−Me^+ system using the 6-31G* basis set and the tight ζ value of 0.003, the CIM subsystem treated by CR-CC(2,3) consisted of 7 central and 24 environment occupied *correlated* orbitals and 199 unoccupied orbitals, spanning 23 atoms depicted in Figure 4. As one can see, the region treated by the higher-level theory X in each X/Y calculation perfectly reflects the corrin conjugation around the cobalt−methyl center. Unlike porhyrins, corrin does not follow the usual Hückel rule,[5] so that one ends up with a partial conjugation of 12 electrons inside the macrocyclic ring around the Co−Me center. It is, therefore, reassuring that our GSECIM algorithm resulted in the active region consistent with this picture.

To make sure that the CCSD/MP2, CR-CC(2,3)/MP2, and CR-CC(2,3)/CCSD energies are reasonably converged with the parameter ζ, each multilevel CC calculation was performed using three increasingly small values of ζ, namely, 0.01, 0.005, and 0.003 (the canonical limit corresponds to $\zeta = 0$). To ensure that the resulting potential energy curves are smooth and that our final CR-CC(2,3)/CCSD BDE calculations do not suffer from the errors due to subsystem rearrangements at larger Co−C_{Me} separations, we invoked the fixed-domain approximation,[40g] which allowed us to force the identical orbital composition of each CIM subsystem at all Co−C_{Me} bond lengths (we used the CIM subsystems obtained at the equilibrium geometry to determine the subsystems at other geometries). Going to larger Co−C_{Me} distances created convergence problems in the underlying canonical CCSD calculations that did not allow us to obtain energies converged to within 10^{-5}−10^{-6} hartree in the $R_{Co-C} > 4.5$ Å region, but, fortunately, we did not have to examine the Co−C_{Me} distances beyond 4.5 Å, since the most accurate dissociation curve resulting from the CR-CC(2,3)/CCSD calculations with $\zeta = 0.003$ becomes flat in that region, enabling us to extract the CR-CC(2,3)/6-311++G**-quality BDE characterizing the Co−C_{Me} bond dissociation in the Im−[Co^{III}corrin]−Me^+ system from the CR-CC(2,3)/CCSD/6-31G* calculations at the $R_{Co-C} = 4.5$ Å and equilibrium geometries, and the analogous canonical CR-CC(2,3)/6-311++G** and CR-CC(2,3)/6-31G* calculations for the $Co(NH_3)_5(Me)^{2+}$ complex, as described in section 2.2 (see section 3.1 for details). Since we had to rely on the RHF-based CC methodology, while maintaining the same orbital composition of the local CIM subsystem in which the Co−C_{Me} bond dissociation takes place at all Co−C_{Me} distances, to guarantee a smooth and balanced description of the PES resulting from the CR-CC(2,3)/CCSD calculations, we could not examine the role of BSSE in our CC-theory-based predictions. However, this is not a problem here, since it is well established that the local correlation size extensive approaches, such as the CIM-based CR-CC(2,3)/CCSD method exploited in this study, efficiently eliminate BSSE, even when the relatively small basis sets are employed.[131]

2.4. CASSCF and CASPT2 Calculations. Since the Co−C_{Me} bond breaking in the Im−[Co^{III}corrin]−Me^+ system is formally a multireference problem, we also attempted the CASSCF[92] and CASPT2[93] calculations. As in the case of the CC and DFT calculations, we were mainly interested in determining the Co−C_{Me} dissociation curve using the selected points along the one-dimensional PES cut obtained in the constrained BP86/6-31G* optimizations. The energies resulting from the largest CASSCF and CASPT2 calculations we could afford do not stabilize in the region of the Co−C_{Me} distances of 4.0−4.5 Å, so we had to consider Co−C_{Me} distances as large as 8.5 Å.

The CASSCF and CASPT2 calculations for the Co−C_{Me} bond dissociation in the Im−[Co^{III}corrin]−Me^+ system were carried out with MOLCAS.[132] Ideally, one would like to use an active space correlating with the valence shells of the Co and methyl group atoms, along with the valence shells of the nitrogen atoms around Co, or, better, valence shells of all of the atoms of the corrin conjugation surrounding Co. Unfortunately, this would lead to a massive active space that would make the

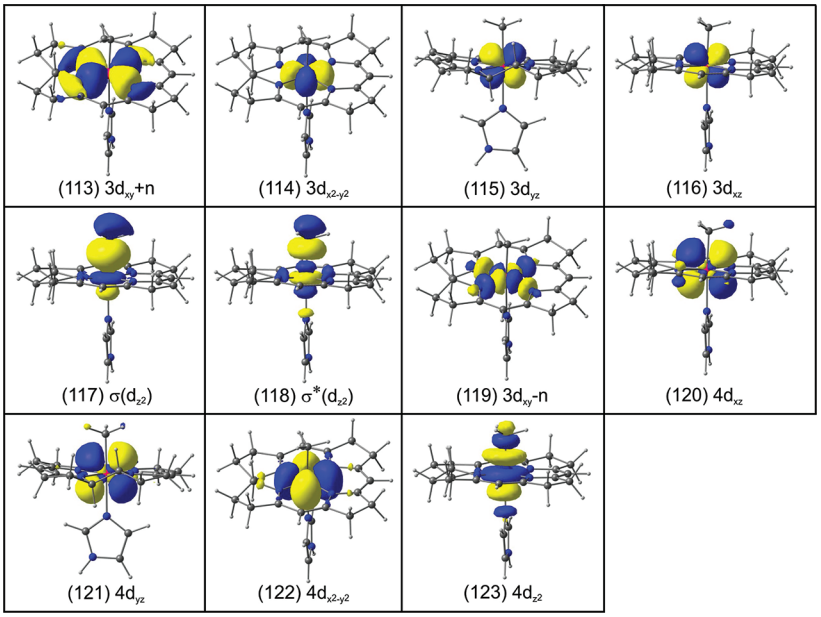

Figure 5. The CASSCF active orbitals used in the CASSCF(11,10) and CASPT2(11,10) calculations for the Im−[Co^{III}corrin]−Me^{+} model of MeCbl using the ANO-S basis set.

CASSCF and CASPT2 calculations unmanageable. Thus, in designing the active space, we had to focus on the smaller subset of valence orbitals that are largely centered on the axial fragment comprised of Co and C_{Me} atoms, restricting the information about the interactions between Co and methyl with the atoms of the corrin conjugation to a minimum. As a result, the active space used in the CASSCF and CASPT2 calculations performed in this study, which were the largest calculations we could afford, contained 10 electrons and 11 orbitals, shown in Figure 5, comprised of the following three orbital subgroups: (i) the doubly occupied $3d_{x^2-y^2}$, $3d_{yz}$, and $3d_{xz}$ orbitals centered on the Co atom, labeled in Figure 5 as orbitals 114−116, and the corresponding 4d-type correlating orbitals, i.e., $4d_{xz}$, $4d_{yz}$, and $4d_{x^2-y^2}$ (in Figure 5, orbitals 120−122), (ii) the bonding Co−C_{Me} $\sigma(d_{z^2})$ orbital and its antibonding $\sigma^*(d_{z^2})$ counterpart (in Figure 5, orbitals 117 and 118, respectively), augmented with the correlating orbital of a $4d_{z^2}$ character to improve the description of the axial binding region (orbital 123 in Figure 5), and (iii) the occupied $3d_{xy}$ + n and unoccupied $3d_{xy}$ − n orbitals resulting from, respectively, the bonding and antibonding combinations of the $3d_{xy}$ orbital centered on the Co atom with the lone pairs (n) centered on four nitrogen atoms around Co (orbitals 113 and 119 in Figure 5). The above active orbitals were selected on the basis of the findings that adding the 4d orbitals as correlating counterparts for the doubly occupied 3d orbitals is important for the calculation of properties of transition metal complexes (the "double shell effect"; see ref 133). This is a standard procedure in the calculations for such systems. The basis set used in the CASSCF(11,10) and CASPT2(11,10) calculations was ANO-S.[134] The ANO-S basis set uses similar contraction schemes to those applied in 6-31G*, namely, 6s5p3d1f for cobalt [5s4p2d1f in the 6-31G* case], 3s2p1d for nitrogen and carbon [3s2p1d in 6-31G*, too], and 2s for hydrogen [2s in 6-31G* as well]. Thus, the ANO-S basis, consisting of 505 functions, is similar to the 6-31G* basis set exploited in the CC and DFT calculations (496 functions). We were unable to extend our CASSCF and CASPT2 calculations to larger basis sets, but we made an attempt to estimate the role of BSSE in the CASSCF(11,10) and CASPT2(11,10) calculations employing the ANO-S basis set.

3. RESULTS AND DISCUSSION

3.1. Reference CC Calculations. As explained in sections 2.2 and 2.3, and considering the enormous computer costs of the CC calculations with the singly, doubly, and triply excited clusters that the CR-CC(2,3) methodology represents, our CC effort, results of which are discussed in this subsection, had to be divided into two stages. In the first stage, the carefully validated multilevel CR-CC(2,3)/CCSD scheme and its CR-CC(2,3)/MP2 and CCSD/MP2 counterparts, all employing the 6-31G* basis set, are used to establish the Co−C_{Me} dissociation curve characterizing the Im−[Co^{III}corrin]−Me^{+} system, which is projected to be within about 1 kcal/mol from the corresponding canonical CR-CC(2,3)/6-31G* curve. The results obtained in this stage enable us to comment on the changes in the nature of the electronic wave function of the Im−[Co^{III}corrin]−Me^{+} system as a function of the Co−C_{Me} distance, to analyze the performance of selected DFT approaches in describing the Co−C_{Me} dissociation curve of Im−[Co^{III}corrin]−Me^{+} and to extract the CR-CC(2,3)/6-31G*-level BDE characterizing the Im−[Co^{III}corrin]−Me^{+} system. In the second stage, the canonical CR-CC(2,3) calculations using the 6-31G* and 6-311++G** basis sets for the $Co(NH_3)_5(Me)^{2+}$ model complex in its lowest-energy singlet state, combined with the ZPE contribution to the Co−C_{Me} BDE in the Im−[Co^{III}corrin]−Me^{+} system obtained with the BP86/6-31G* approach, are used to extrapolate the CR-CC(2,3)/CCSD/6-311++G** result for the Co−C_{Me} BDE in Im−[Co^{III}corrin]−Me^{+}, which cannot be obtained in a direct calculation due to prohibitive computer costs.

We begin our discussion with the first stage, in which a series of the CCSD/MP2, CR-CC(2,3)/MP2, and CR-CC(2,3)/CCSD calculations using different values of the CIM parameter ζ and the 6-31G* basis set, at the selected points along the one-dimensional PES cut in the R_{Co-C} = 1.969−4.5 Å

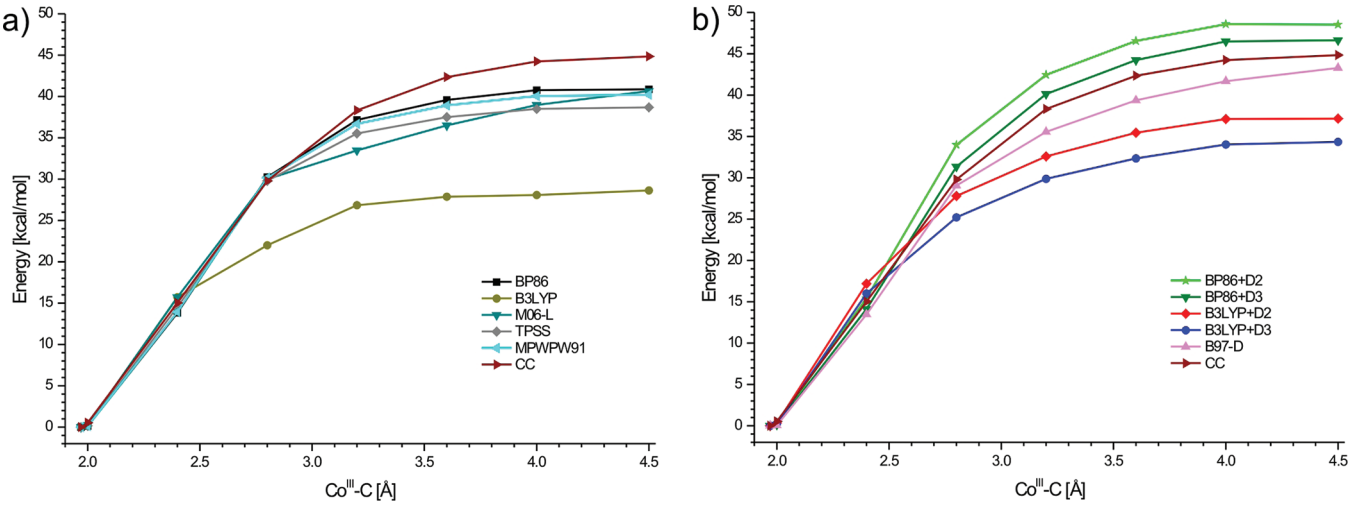

Figure 6. A comparison of the Co−C_{Me} bond dissociation curves for the Im−[Co^{III}corrin]−Me^+ system computed using a few representative DFT methods, without (a) and with (b) dispersion corrections, with the reference CC curve resulting from the multilevel CR-CC(2,3)/CCSD calculation with ζ = 0.003, where the relevant single-point calculations were performed at the selected geometries along the one-dimensional PES cut obtained in the constrained BP86 optimizations. The 6-31G* basis set was employed throughout.

region, obtained in the constrained BP86/6-31G* geometry optimizations, was used to determine the benchmark, CR-CC(2,3)/6-31G*-level, potential curve for the Co−C_{Me} dissociation in the Im−[Co^{III}corrin]−Me^+ molecule. The final potential energy curve of this type, shown in Figure 6, was obtained in the CR-CC(2,3)/CCSD calculations with ζ = 0.003 (the ζ value recommended for high-accuracy CIM-CC calculations using the GSECIM algorithm[47,48]). The analysis below explains why we can regard this curve as a reference curve for assessing the performance of other methods and for extracting the CR-CC(2,3)/6-31G*-level BDE value.

First, we demonstrate that our selection of the CIM subsystem, which represents the active region of the Im−[Co^{III}corrin]−Me^+ model of MeCbl where the Co−C_{Me} bond dissociation occurs, shown in Figure 4, and our final choice of the CIM parameter ζ (0.003) are appropriate for making a claim that, by describing the bulk of the correlation energy in the active and inactive regions using one of the affordable canonical *ab initio* methods (ultimately in this work, CCSD) and by employing the local CC approach to capture the higher-order correlation effects in the active region [ultimately, CR-CC(2,3)], one obtains a reliable representation of the corresponding canonical CC potential energy curve for the Co−C_{Me} bond dissociation in Im−[Co^{III}corrin]−Me^+. Since canonical CR-CC(2,3) calculations for the Im−[Co^{III}corrin]−Me^+ system could not be performed, our assessment of the ability of the multilevel CIM-CC methodology to reproduce the corresponding canonical CC results is based on comparing the CCSD/MP2 and canonical CCSD calculations, both exploiting the same 6-31G* basis set. Let us recall that the CCSD/MP2 method describes the bulk of the correlation energy in the active and inactive regions at the canonical MP2 level, while using local CCSD to capture the higher-order correlation effects originating from the active region neglected in MP2.

The results of this comparison, corresponding to three different choices of the CIM parameter ζ approaching the canonical ζ = 0 limit, are shown in Table 1. As we can see, one has to consider ζ of 0.005 or less to obtain an accurate representation of the corresponding canonical CC (in this case,

Table 1. A Comparison of the Electronic Energies of the Im−[Co^{III}corrin]−Me^+ System Obtained with Canonical MP2, Canonical CCSD, and the Multilevel CIM Approach Mixing Local CCSD with Canonical MP2 (CCSD/MP2), Using the 6-31G* Basis Set, at Selected Values of the Co−C_{Me} Distance R_{Co-C} (in Å), Relative to the Energy Values Obtained at the Equilibrium (R_{Co-C} = 1.969 Å) Geometry Resulting from the BP86/6-31G* Calculations[a]

			CCSD/MP2		
R_{Co-C}	MP2	CCSD	ζ = 0.01	ζ = 0.005	ζ = 0.003
1.969	0.00	0.00	0.00	0.00	0.00
2.00	1.50	0.76	1.05	0.74	0.88
2.40	24.47	17.52	17.84	16.59	16.41
2.80	49.05	35.80	35.99	33.44	33.45
3.20	68.65	47.83	49.55	45.63	45.66
3.60	84.76	55.09	60.11	54.60	54.78
4.00	96.70	59.30	67.16	60.19	60.28
4.50	105.13	61.87	71.80	63.23	63.30
MUE[b]	21.73	0.00	3.62	1.18	1.21
NPE[c]	43.26	0.00	9.93	2.36	2.35

[a]All energies are in kcal/mol. [b]Mean unsigned error relative to canonical CCSD using the results obtained at R_{Co-C} = 2.0, 2.4, 2.8, 3.2, 3.6, 4.0, and 4.5 Å. [c]Nonparallelity error relative to canonical CCSD using the results obtained at R_{Co-C} = 2.0, 2.4, 2.8, 3.2, 3.6, 4.0, and 4.5 Å.

CCSD) potential energy curve. The mean unsigned error (MUE) relative to canonical CCSD characterizing the CCSD/MP2 calculations using ζ = 0.003 and ζ = 0.005 at the eight points along the Co−C_{Me} bond breaking curve of Im−[Co^{III}corrin]−Me^+ listed in Table 1 is about 1 kcal/mol, which gives excellent agreement between the CCSD/MP2 and canonical CCSD results. The corresponding nonparallelity error (NPE), defined as the difference between the maximum and minimum signed errors in the CCSD/MP2 energies relative to canonical CCSD along the Co−C_{Me} bond breaking coordinate, of about 2 kcal/mol, is very small as well. This shows that choosing $\zeta \leq 0.005$ enables one to recover canonical CC results to within about 1−2 kcal/mol by using the corresponding multilevel CC/MP2 method. One cannot rely

Table 2. A Comparison of the Electronic Energies of the Im−[Co^{III}corrin]−Me$^+$ System Obtained with Canonical MP2, Canonical CCSD, and the Multilevel CIM Approaches Mixing Local CR-CC(2,3) with Canonical MP2 [CR-CC(2,3)/MP2] and CCSD [CR-CC(2,3)/CCSD], Using the 6-31G* Basis Set, at Selected Values of the Co−C Distance R_{Co-C} (in Å), Relative to the Energy Values Obtained at the Equilibrium (R_{Co-C} = 1.969 Å) Geometry Resulting from the BP86/6-31G* Calculations[a]

			CR-CC(2,3)/MP2			CR-CC(2,3)/CCSD		
R_{Co-C}	MP2	CCSD	ζ = 0.01	ζ = 0.005	ζ = 0.003	ζ = 0.01	ζ = 0.005	ζ = 0.003
1.969	0.00	0.00	0.00	0.00	0.00	0.00	0.00	0.00
2.00	1.50	0.76	0.90	0.51	0.66	0.61	0.53	0.53
2.40	24.47	17.52	14.86	14.21	13.92	14.53	15.14	15.02
2.80	49.05	35.80	28.98	27.15	27.46	28.79	29.51	29.80
3.20	68.65	47.83	38.97	36.07	36.15	37.25	38.27	38.31
3.60	84.76	55.09	46.51	41.75	42.04	41.49	42.24	42.35
4.00	96.70	59.30	51.20	45.07	45.21	43.34	44.18	44.23
4.50	105.13	61.87	55.05	46.12	46.29	45.11	44.76	44.85

[a]All energies are in kcal/mol.

on the loose ζ values, such as ζ = 0.01, which would lead to substantial additional savings in the computer effort, to obtain an accurate representation of the corresponding canonical CC potential energy curve within the CC/MP2 context. As shown in Table 1, the MUE and NPE values relative to canonical CCSD characterizing the CCSD/MP2 dissociation curves obtained with ζ = 0.01 are about 4 and 10 kcal/mol, respectively, i.e., they are too large to be acceptable. On the other hand, using very tight ζ < 0.003 values, which, being closer to the canonical ζ = 0 limit, would allow us to recover the corresponding canonical energetics to within small fractions of kcal/mol, would make the final CR-CC(2,3)/CCSD calculations too expensive for our computers, considering the size of the Im−[Co^{III}corrin]−Me$^+$ system, even when the 6-31G* basis set is employed. The ζ = 0.003 value offers us an excellent compromise between high accuracy and relatively low computer cost, allowing us to obtain the CR-CC(2,3)/MP2 and CR-CC(2,3)/CCSD potential energy curves, which, based on the CCSD/MP2 results shown in Table 1, should remain within ∼1−2 kcal/mol from the corresponding canonical CR-CC(2,3)/6-31G* curve, in a few days per structure on the PES.

Another manifestation of the appropriateness of this particular choice of ζ and of the active region of the Im−[Co^{III}corrin]−Me$^+$ model of MeCbl, depicted in Figure 4, that this choice leads to is the examination of the largest singly excited (T_1) and doubly excited (T_2) cluster amplitudes resulting from the canonical vs local CCSD calculations, particularly when the Co−C$_{Me}$ bond is stretched. For example, the largest T_1 and T_2 amplitudes in the canonical CCSD/6-31G* calculation at the significantly stretched R_{Co-C} = 3.6 Å geometry, corresponding to the single and double excitations from the Co−C$_{Me}$ $\sigma(d_{z^2})$ bonding to the $\sigma^*(d_{z^2})$ antibonding orbitals, are 0.593 and −0.625, respectively, demonstrating the predominantly $\sigma(d_{z^2})\rightarrow\sigma^*(d_{z^2})$ nature of the Co−C$_{Me}$ bond dissociation in MeCbl (for comparison, the largest T_1 and T_2 amplitudes at the equilibrium geometry do not exceed, in absolute value, 0.133 and 0.060, respectively). The analogous T_1 and T_2 amplitudes resulting from the local CCSD/6-31G* calculation in the CIM subsystem representing the active region of Im−[Co^{III}corrin]−Me$^+$ shown in Figure 4 are 0.588 and −0.622, respectively, when the quasi-canonical MO basis is employed to describe it, in perfect agreement with the corresponding canonical CCSD calculation for the entire system (the quasi-canonical MO basis is a local analog of the canonical RHF basis limited to a specific CIM subsystem; see refs 46−48 for details). Similar remarks apply to other Co−C$_{Me}$ bond lengths and other larger cluster amplitudes, confirming that our final choice of ζ and of the resulting active region of the Im−[Co^{III}corrin]−Me$^+$ system where the Co−C$_{Me}$ bond dissociation occurs are appropriate, reflecting on the underlying chemistry of Im−[Co^{III}corrin]−Me$^+$ in a physically meaningful manner.

Now that we have established a reasonable choice of ζ, we examine the results obtained with the CR-CC(2,3)/MP2 and CR-CC(2,3)/CCSD methods, shown in Table 2, which both improve the description of the active region of the Im−[Co^{III}corrin]−Me$^+$ system via robust noniterative corrections to CCSD energies due to connected triple excitations obtained with CR-CC(2,3). Again, the 6-31G* basis set is employed throughout. Unlike CCSD, the CR-CC(2,3) approach provides a fully quantitative description of single bond breaking,[88,89] so, based on the above analysis of the local CCSD/MP2 vs canonical CCSD calculations, we can immediately claim that the analogous CR-CC(2,3)/MP2 calculations using ζ = 0.003 provide an accurate representation of the Co−C$_{Me}$ bond dissociation curve for Im−[Co^{III}corrin]−Me$^+$ that should stay within about 1−2 kcal/mol from the corresponding canonical CR-CC(2,3) curve. We can further improve the already accurate CR-CC(2,3)/MP2 results obtained with ζ = 0.003 by replacing the canonical MP2 approach, as a way to capture the bulk of the electron correlation effects in the entire system within the multilevel CIM-CC methodology, by the canonical CCSD calculations, reducing the portion of the correlation energy that has to be treated at the local CIM level to the relatively small triples corrections to CCSD energies [as opposed to the considerably larger difference between the MP2 and CR-CC(2,3) correlation energies treated locally within the CR-CC(2,3)/MP2 scheme]. Since the CR-CC(2,3)/MP2 potential energy curve obtained with ζ = 0.003 is estimated to lie within 1−2 kcal/mol from the corresponding canonical CR-CC(2,3) curve and since the canonical CCSD approach reproduces a significantly larger fraction of the total correlation energy than MP2, we can expect that the ζ = 0.003 CR-CC(2,3)/CCSD curve is practically identical (to within a fraction of kcal/mol) to the canonical CR-CC(2,3) curve. The results in Table 2 confirm this expectation, since the CR-CC(2,3)/CCSD results obtained with the relatively tight ζ = 0.003 threshold are no longer significantly different than those obtained with the much larger ζ value of 0.01 (at most 1 kcal/mol differences). A comparison of the CR-CC(2,3)/CCSD energies obtained with ζ = 0.01, 0.005, and 0.003, where the differences between the ζ = 0.01 and ζ = 0.005 energies are

Table 3. A Comparison of the Co−C_{Me} and Co−N_{Im} Bond Lengths (in Å) and the ZPE- and BSSE-Corrected BDE Values (in kcal/mol) for the Im−[Co^{III}corrin]−Me^+ System, Obtained with Various DFT Approaches, and the ZPE-Corrected CR-CC(2,3)/CCSD BDE Values with the Available Experimental Data

			6-31G*			6-311++G**[b]	
method[a]	Co−C_{Me}	Co−N_{Im}	ZPE	BSSE	BDE	BSSE	BDE
BHandHLYP (50% HF)	1.934	2.158	5.9	5.2	1.2	1.0	−2.2
MPW1K (42.8% HF)	1.921	2.107	5.7	5.2	8.9	1.2	6.0
M06-2X (54% HF)	1.932	2.141	5.7	5.4	13.5	1.0	9.2
MPW1PW91 (25% HF)	1.935	2.121	5.5	5.8	18.1	1.2	16.1
B3LYP (20% HF)	1.956	2.179	5.4	6.2	17.8	1.0	15.9
B3LYP+D2 (20% HF, DFT-D2)[c]	1.956	2.096			29.8[d]		27.8[d]
B3LYP+D3 (20% HF, DFT-D3)[e]	1.956	2.169			21.2[d]		24.7[d]
M06 (27% HF)	1.944	2.119	5.7	6.7	27.4	1.3	26.2
OLYP	1.965	2.354	5.0	6.6	20.3	1.1	20.0
TPSSh (10% HF)	1.951	2.114	5.3	5.8	24.5	1.2	23.0
ωB97X-D (22% HF)	1.938	2.120	5.5	5.8	26.8	1.1	24.8
BLYP	1.989	2.210	5.1	7.0	25.7	1.0	24.8
TPSS	1.965	2.119	5.1	6.0	29.1	1.2	28.1
MPWPW91	1.967	2.139	5.1	6.5	30.3	1.2	29.7
M06-L	1.955	2.142	5.7	5.5	31.3	1.3	29.8
BP86	1.969	2.130	5.1	6.4	30.6	1.1	30.0
BP86+D2 (DFT-D2)[c]	1.967	2.064			40.4[f]		41.1[f]
BP86+D3 (DFT-D3)[e]	1.968	2.115			35.2[f]		39.7[f]
B97-D	1.978	2.116	5.3	5.9	35.1	1.2	34.8
CR-CC(2,3)/CCSD					39.8[g]		37.8[i]
CR-CC(2,3)/CCSD					39.5[h]		37.5[i]
experiment	1.97[j]	2.09[k]			37 ± 3,[l] 36 ± 4[m]		

[a]For each DFT hybrid functional, percentage of the HF exchange has been listed in parentheses. [b]ZPE corrections from calculations with the 6-31G* basis set. [c]Calculations with "+D2" dispersion correction of ref 100b. [d]BDE values corrected for the ZPE and BSSE contributions obtained in the B3LYP calculations without dispersion corrections. [e]Calculations with "+D3" dispersion correction of ref 100c. [f]BDE values corrected for the ZPE and BSSE contributions obtained in the BP86 calculations without dispersion corrections. [g]Obtained using the electronic energy difference $E(R_{Co-C} = 4.5\ Å) - E(R_{Co-C,e})$ resulting from the multilevel CR-CC(2,3)/CCSD calculations with the 6-31G* basis set and $\zeta = 0.003$, where $R_{Co-C,e}$ represents the equilibrium geometry of the Im−[Co^{III}corrin]−Me^+ system obtained in the BP86/6-31G* calculations, and corrected for ZPE using the BP86/6-31G* ZPE value. [h]Obtained using the electronic energy difference $E(R_{Co-C} = 4.5\ Å) - E(R_{Co-C,e})$ resulting from the multilevel CR-CC(2,3)/CCSD calculations with the 6-31G* basis set and $\zeta = 0.003$, where $R_{Co-C,e}$ represents the equilibrium geometry of the Im−[Co^{III}corrin]−Me^+ system obtained in the BP86/6-31G* calculations, and corrected for ZPE using the average DFT ZPE value. [i]Estimated by adding the difference between the electronic BDEs resulting from the canonical CR-CC(2,3)/6-311++G** and CR-CC(2,3)/6-31G* calculations for the $Co(NH_3)_5(Me)^{2+}$ model complex to the ZPE-corrected BDE obtained in the CR-CC(2,3)/CCSD/6-31G* calculations for the Im−[Co^{III}corrin]−Me^+ molecule using $\zeta = 0.003$. [j]Experimental Co−C_{Me} distance from ref 112. [k]Experimental Co−N_{Im} distance from ref 112. [l]Co−C_{Me} BDE based on thermolysis in ethylene glycol, ref 22. [m]Co−C_{Me} BDE based on photoacoustic calorimetry, ref 23.

within ∼1 kcal/mol and those between the $\zeta = 0.005$ and $\zeta = 0.003$ energies within ∼0.3 kcal/mol, demonstrates that the Co−C_{Me} bond dissociation curve obtained in the CR-CC(2,3)/CCSD calculations with $\zeta = 0.003$ and the 6-31G* basis set can be regarded as virtually converged, as far as electron correlation effects are concerned, and for all practical purposes equivalent to the analogous canonical CR-CC(2,3)/6-31G* curve.

For all of the above reasons and considering the fact that the CR-CC(2,3) theory is known to provide high-quality PESs for single bond breaking, the electronic energies resulting from the CR-CC(2,3)/CCSD/6-31G* calculations with $\zeta = 0.003$, shown in Table 2 and Figure 6, provide a solid basis for assessing the performance of other (particularly, DFT) methods. They also enable us to determine the CR-CC(2,3)-level benchmark information about the Co−C_{Me} BDE in Im−[Co^{III}corrin]−Me^+ by forming the difference of the CR-CC(2,3)/CCSD/6-31G* energies obtained with $\zeta = 0.003$ at the $R_{Co-C} = 4.5$ Å and equilibrium geometries, which we subsequently correct for the ZPE contributions resulting from the BP86/6-31G* calculations and the effects of going from the smaller 6-31G* to the larger 6-311++G** basis estimated by examining the $Co(NH_3)_5(Me)^{2+}$ model complex, in spite of having no direct access to the CR-CC(2,3)/CCSD data beyond $R_{Co-C} = 4.5$ Å. We did not have to examine the Co−C_{Me} distances beyond 4.5 Å, since our best dissociation curve for Im−[Co^{III}corrin]−Me^+ resulting from the CR-CC(2,3)/CCSD/6-31G* calculations with $\zeta = 0.003$ becomes flat in that region. Indeed, as shown in Table 2, the CR-CC(2,3)/CCSD energies of the Im−[Co^{III}corrin]−Me^+ system obtained with $\zeta = 0.003$ and the 6-31G* basis set change by 0.6 kcal/mol only, when the Co−C_{Me} distance increases from 4.0 to 4.5 Å, as opposed to 2.1 and 4.0 kcal/mol, when R_{Co-C} changes from 3.6 to 4.0 and 3.2 to 3.6 Å, respectively, i.e., they rapidly stabilize as we approach the $R_{Co-C} = 4.5$ Å region. Another indication of the flatness of the $\zeta = 0.003$ CR-CC(2,3)/CCSD PES in the region of the Co−C_{Me} distances of 4.5 Å or more is the very small, ∼1 kcal/mol, difference between the BP86/6-31G* energies at $R_{Co-C} = 4.5$ Å and $R_{Co-C} = \infty$, where the latter energy can be determined from the information about the noninteracting Im−[Co^{II}corrin]$^+$ and Me fragments [as shown in Figure 6, the $\zeta = 0.003$ CR-CC(2,3)/CCSD and BP86 PESs resulting from the calculations with the 6-31G* basis set have similar overall shapes, particularly at larger Co−

C_{Me} separations]. We should also add that we are much better off by estimating the CR-CC(2,3)-level BDE in the Im−[Co^{III}corrin]−Me^+ system from the well-behaved CR-CC(2,3)/CCSD energies obtained with ζ = 0.003 at the R_{Co-C} = 4.5 Å and equilibrium geometries rather than from the CR-CC(2,3)/CCSD information about the open-shell dissociation fragments (Im−[Co^{II}corrin]$^+$ and methyl). Indeed, according to our analysis, trying to determine the CR-CC(2,3)/CCSD BDE value using the CR-CC(2,3)/CCSD energies of the Im−[Co^{II}corrin]$^+$ and methyl fragments leads to substantial errors due to the significant local domain rearrangements when switching from the entire Im−[Co^{III}corrin]−Me^+ system (treated as a single molecule in which the Co−C_{Me} bond is broken) to the dissociation fragments, which result in much larger uncertainties than those characterizing the ζ = 0.003 CR-CC(2,3)/CCSD energy and BDE values listed in Tables 2 and 3. The fixed-domain CR-CC(2,3)/CCSD calculations up to R_{Co-C} = 4.5 Å using ζ = 0.003, in which we treat the dissociating Im−[Co^{III}corrin]−Me^+ molecule as a single system, do not suffer from any of these problems, while enabling us to obtain reliable information about the Co−C_{Me} bond breaking curve (Table 2 and Figure 6) and the corresponding BDE (Table 3).

On the basis of the flatness of the PES in the R_{Co-C} = 4.5 Å region and on the basis of the proximity of the canonical CC and multilevel CIM-CC energies obtained with ζ = 0.003, and the stability of the CR-CC(2,3)/CCSD/6-31G* energies with respect to ζ, as analyzed above, we can assume that the BDE calculated as $E(R_{Co-C}$ = 4.5 Å) − $E(R_{Co-C,e})$, where $E(R_{Co-C}$ = 4.5 Å) and $E(R_{Co-C,e})$ are the CR-CC(2,3)/CCSD/6-31G* energies of the Im−[Co^{III}corrin]−Me^+ system at the R_{Co-C} = 4.5 Å and equilibrium geometries, respectively, using ζ = 0.003 is within ∼1−2 kcal/mol from the corresponding canonical CR-CC(2,3)/6-31G* result. After correcting the electronic CR-CC(2,3)/CCSD/6-31G* BDE obtained with ζ = 0.003 for the Im−[Co^{III}corrin]−Me^+ system for the ZPE contribution resulting from the BP86/6-31G* calculations, we obtain the value of 39.8 kcal/mol, which falls within the error bars of the experimental BDE values obtained in refs 22 and 23 (see Table 3). This result could change if we used a different functional to determine the ZPE contribution, but not by much. For example, if we replace the BP86/6-31G* ZPE correction by the average of all DFT ZPE values obtained in this study, the estimated ZPE-corrected CR-CC(2,3)/CCSD/6-31G* BDE changes to 39.5 kcal/mol (cf. Table 3). As discussed in section 3.2, the ZPE corrections are rather insensitive to the DFT functional.

The CR-CC(2,3)/CCSD dissociation curve shown in Figure 6 and the ZPE-corrected BDE value resulting from the CR-CC(2,3)/CCSD calculations with ζ = 0.003 and the 6-31G* basis set are useful for assessing the results of other quantum chemistry calculations, particularly those using basis sets of similar quality, but in order to make our analysis more quantitative it is important to estimate the effect of the basis set on the Co−C_{Me} dissociation energy in the Im−[Co^{III}corrin]−Me^+ system resulting from our best CR-CC(2,3)/CCSD calculations. This is important, since the highly correlated wave function methods of the CR-CC(2,3) type and the DFT approaches, which we are comparing here, have different requirements for reaching the basis-set limit. Thus, we would like to know how the CR-CC(2,3)/CCSD BDE value obtained with ζ = 0.003 and the 6-31G* basis set would change if we replaced 6-31G* with a larger basis set of the triple-zeta plus polarization and diffuse function quality, such as, for example, 6-311++G**. Unfortunately, as pointed out in section 2, the CR-CC(2,3)/CCSD calculations for the Im−[Co^{III}corrin]−Me^+ system using the 6-311++G** basis set and the sufficiently tight ζ values that would guarantee the desired ∼1 kcal/mol accuracy relative to the corresponding canonical CR-CC(2,3) data are prohibitively expensive. Thus, in analogy to ref 97, to estimate the effect of the basis set on the Co−C_{Me} dissociation energy in the Im−[Co^{III}corrin]−Me^+ system resulting from the CR-CC(2,3)/CCSD/6-31G* calculations, we performed the canonical CR-CC(2,3)/6-31G* and CR-CC(2,3)/6-311++G** calculations for the related $Co(NH_3)_5(Me)^{2+}$ model complex[108] in its lowest singlet state, as described in section 2.2. The results of these auxiliary calculations are summarized in Table 4. As we can see, the effect of the basis set, when moving from 6-31G* to 6-311++G**, on the CR-CC(2,3)-level data, particularly in the region of larger Co−C_{Me} separations that affect the BDE calculations, is relatively small, demonstrating that the CR-CC(2,3)/CCSD/6-31G* dissociation curve obtained for the Im−[Co^{III}corrin]−Me^+ molecule carries useful information, at least for a qualitative examination of various quantum chemistry methods. The basis set effect is largest in the region of intermediate Co−C_{Me} distances around 3.0 Å, approaching the ∼4 kcal/mol range for the relative energy lowering that results when we replace the 6-31G* basis set by 6-311++G**, and settles down at about 2 kcal/mol as we approach the R_{Co-C} = 4.5 Å limit. Thus, the extrapolated CR-CC(2,3)/CCSD/6-311++G** results for the BDE characterizing the Co−C_{Me} dissociation in the Im−[Co^{III}corrin]−Me^+ system, obtained by adding the difference between the BDEs resulting from the canonical CR-CC(2,3)/6-311++G** and CR-CC(2,3)/6-31G* calculations for the $Co(NH_3)_5(Me)^{2+}$ complex, of about (−2) kcal/mol, to the ZPE-corrected BDEs obtained in the CR-CC(2,3)/CCSD calculations for the Im−[Co^{III}corrin]−Me^+ molecule using ζ = 0.003 and the 6-31G* basis set, is ∼37.8 kcal/mol, when we use the BP86/6-31G* ZPE value, and ∼37.5 kcal/mol, when we use an average of all DFT ZPE values obtained in this study instead (see Table 3). Both of these estimates are in very good agreement with the available experimental values characterizing the MeCbl cofactor of 37 ± 3 and 36 ± 4 kcal/mol.[22,23] We realize the approximate nature

Table 4. A Comparison of the Canonical CR-CC(2,3)/6-31G* and CR-CC(2,3)/6-311++G Energies of the $Co(NH_3)_5(Me)^{2+}$ Model Complex at Selected Values of the Co−C_{Me} Distance R_{Co-C} (in Å), Relative to the Energy Values Obtained at the Equilibrium (R_{Co-C} = 1.9575 Å) Geometry Resulting from the BP86/6-31G* Calculations[a]**

R_{Co-C}	6-31G*	6-311++G**	change[b]
1.9575	0.00	0.00	0.00
2.20	5.34	3.82	−1.52
2.40	13.35	10.75	−2.60
2.60	20.94	17.17	−3.77
2.80	26.62	22.56	−4.06
3.00	30.70	26.67	−4.03
3.50	36.06	33.58	−2.48
4.00	38.53	36.68	−1.85
4.50	40.10	38.07	−2.03

[a]All energies are in kcal/mol. [b]The difference between the CR-CC(2,3)/6-311++G** and CR-CC(2,3)/6-31G* energies, calculated relative to their equilibrium values.

of the above analysis and of all of the assumptions that are part of it, but considering the well-established ability of the CR-CC(2,3) approach to achieve chemical (~1 kcal/mol) accuracy in describing single bond breaking when larger basis sets of triple-zeta plus polarization and diffuse function quality are employed (or when compared with full CI in smaller basis set calculations), combined with the fact that the BDEs resulting from our best CR-CC(2,3)/CCSD/6-31G* calculations with ζ = 0.003 are estimated to be within ~1 kcal/mol from the corresponding canonical CR-CC(2,3) result, it is safe to assume that the extrapolated CR-CC(2,3)/CCSD/6-311++G** BDE values shown in Table 3, which fall into the 37−38 kcal/mol range, are accurate to within 2−3 kcal/mol or so. By the same token, considering the relatively small dependence of the CR-CC(2,3)-level description of the Co−C_{Me} dissociation curve on the basis set, shown in Table 4, we can regard the ζ = 0.003 CR-CC(2,3)/CCSD/6-31G* potential energy curve shown in Figure 6 and Table 2 to be converged to within about 4−5 kcal/mol or so. Considering the additional facts that the CR-CC(2,3) single bond breaking curves are typically above the corresponding full CI-level potentials (cf., e.g., ref 89d, e), that the use of the larger basis sets lowers the CR-CC(2,3) energies (cf. Table 4), and that the use of the multilevel CIM-CC methodology produces relative energies above the corresponding canonical energy values (cf. Table 1), we may expect that the extrapolated CR-CC(2,3)/CCSD/6-311++G** BDE values shown in Table 3 of about 38 kcal/mol are somewhat (~2−3 kcal/mol) above their converged counterparts. Similarly, we can expect that the CR-CC(2,3)/CCSD/6-31G* potential energy curve obtained with ζ = 0.003, shown in Figure 6 and Table 2, dissociates at somewhat (~4−5 kcal/mol) too high an energy compared to its converged counterpart. All of this implies that the BDE of the isolated Im−[Co^{III}corrin]−Me^+ system is, quite likely, in the ~35−38 kcal/mol range, so that the DFT and DFT+D methods (and other quantum chemistry approaches) which produce BDE values that are considerably outside this range should not be recommended for calculations for cobalamins or at least used with caution. The fact that the CR-CC(2,3)/6-311++G**-level BDE values characterizing the isolated Im−[Co^{III}corrin]−Me^+ molecule are so close to the experimental dissociation energies characterizing the MeCbl system reported in refs 22 and 23 also indicates that the solvation and thermal effects, which contribute to the experimentally determined BDEs, but do not enter the calculations for the isolated Im−[Co^{III}corrin]−Me^+ system considered in this work, cannot play a major role.

Before discussing the DFT and CASSCF/CASPT2 results, let us return to the issue of the largest singly and doubly excited cluster amplitudes characterizing our CC calculations for the Im−[Co^{III}corrin]−Me^+ system. The above example of the dominant T_1 and T_2 amplitudes at R_{Co-C} = 3.6 Å shows that the configuration state function corresponding to the single $\sigma(d_{z^2})\rightarrow\sigma^*(d_{z^2})$ excitation begins to play a significant role at the considerably shorter Co−C_{Me} distances when compared to the CASSCF(11,10) and CASPT2(11,10) calculations discussed in section 3.3. The canonical and local CC calculations for the Im−[Co^{III}corrin]−Me^+ species performed in this work clearly indicate the large significance of the single as well as double excitations of the $\sigma(d_{z^2})\rightarrow\sigma^*(d_{z^2})$ type at the Co−C_{Me} distances as small as 3.2 Å, where the absolute values of the corresponding T_1 and T_2 amplitudes obtained with the canonical CCSD approach are already 0.488 and 0.487, respectively, when the 6-31G* basis set is employed. The presence of the relatively large single excitations of the $\sigma(d_{z^2})\rightarrow\sigma^*(d_{z^2})$ type in the CC wave functions at Co−C_{Me} distances as small as 3.2 Å, in addition to the equally important double $\sigma(d_{z^2})\rightarrow\sigma^*(d_{z^2})$ excitations, helps the CR-CC(2,3)/CCSD calculations reach the near-asymptotic energy values corresponding to the dissociation fragments already in the $R_{Co-C} \approx$ 4.0−4.5 Å region, as opposed to the $R_{Co-C} \approx$ 8.0−8.5 Å distances needed to accomplish the same within the CASSCF(11,10)/CASPT2(11,10) framework (see Figure 7).

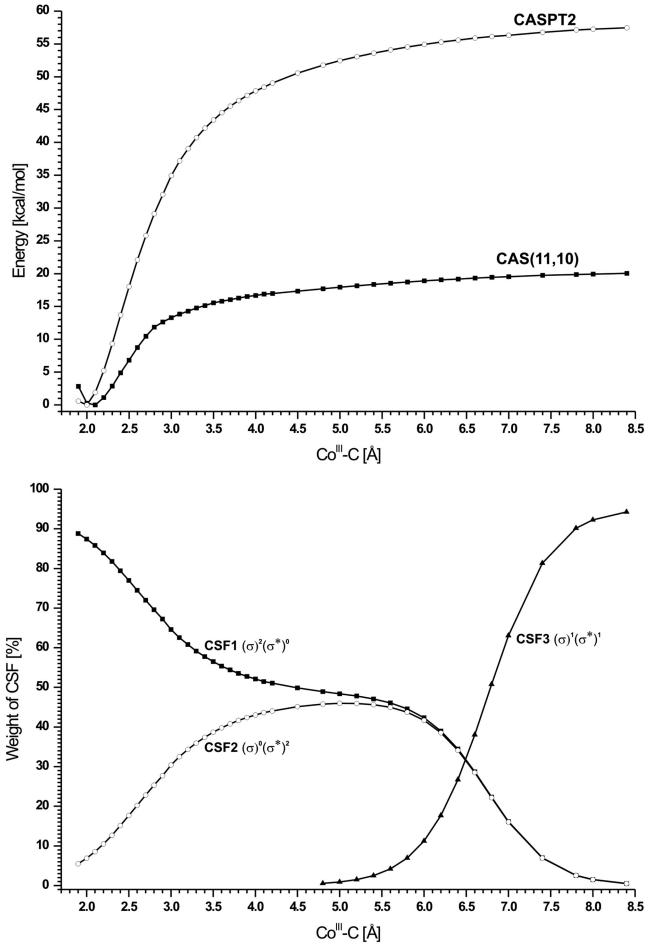

Figure 7. Upper panel: The Co−C_{Me} bond dissociation curves for the Im−[Co^{III}corrin]−Me^+ model of MeCbl computed using the CASSCF(11,10) and CASPT2(11,10) methods employing the ANO-S basis set (the relevant single-point calculations were performed at the selected geometries along the one-dimensional PES cut obtained in the constrained BP86/6-31G* optimizations). Lower panel: weight percentage of the three most important configuration state functions (CSFs) in the CASSCF wave function as a function of the Co−C_{Me} bond length. The increase of the CSF3 weight and the decrease of the CSF1 and CSF2 weights correspond to a progressive localization of the $\sigma(d_{z^2})$ and $\sigma^*(d_{z^2})$ orbitals on the atomic $p_z(C_{Me})$ and d_{z^2}(Co) orbitals.

The additional important effect that helps the CR-CC(2,3)/CCSD dissociation curve stabilize at shorter Co−C_{Me} distances when compared with CASSCF(11,10)/CASPT2(11,10) is the fast growing significance of the single and double excitations from the Co−C_{Me} bonding $\sigma(d_{z^2})$ orbital to the lowest-energy unoccupied orbital mixing the antibonding $\sigma^*(d_{z^2})$ character with the delocalized network of p_z orbitals of the in-plane nitrogen and carbon atoms around

Co, which reflects on the corrin conjugation around the cobalt center, in the CC wave functions, as the Co−C_{Me} bond is stretched. For example, the absolute values of the two largest T_1 amplitudes in the canonical CCSD/6-31G* calculation for the Im−[Co^{III}corrin]−Me^+ system at R_{Co-C} = 4.0 Å that correspond to single excitations from the Co−C_{Me} bonding $\sigma(d_{z^2})$ orbital to the antibonding $\sigma^*(d_{z^2})$ orbital and from the $\sigma(d_{z^2})$ orbital to the lowest-energy orbital having the aforementioned mixed character, designated here as φ, are 0.609 and 0.386, respectively. The absolute values of the three largest T_2 amplitudes resulting from the canonical CCSD/6-31G* calculation at the same Co−C_{Me} distance and corresponding to the double $\sigma(d_{z^2})\rightarrow\sigma^*(d_{z^2})$ excitation, the double excitation from the Co−C_{Me} bonding $\sigma(d_{z^2})$ orbital to the $\sigma^*(d_{z^2})$ and φ orbitals, and the double $\sigma(d_{z^2})\rightarrow\varphi$ excitation are 0.594, 0.415, and 0.296, respectively. The analogous local CCSD/6-31G* calculation in the CIM subsystem representing the active region of Im−[Co^{III}corrin]−Me^+ give, for the same two T_1 and the same three T_2 amplitudes, 0.613, 0.388, 0.609, 0.418, and 0.291, respectively, again in very good agreement with the canonical CCSD results. All of these additional excitations help the CR-CC(2,3)/CCSD approach provide an accurate description of the Co−C_{Me} dissociation curve, which results in the BDE estimates that fall within the experimental error bars. None of these excitations are significant in the CASSCF(11,10) and CASPT2(11,10) wave functions at the Co−C_{Me} distances in the $R_{Co-C} \approx 4.0-4.5$ Å region, and this contributes to the difficulties the CASSCF(11,10) and CASPT2(11,10) approaches have with providing reasonable Co−C_{Me} dissociation curves and BDE values discussed in section 3.3 and illustrated in Figure 7, largely due to the inadequacy of the active space used in the CASSCF(11,10) and CASPT2(11,10) calculations, which was the largest active space we could afford but not large enough.

3.2. Comparison of DFT with Experiment and Reference CC Results. We begin by discussing the Co−C_{Me} BDE data based on determining the geometries, electronic energies, and ZPEs of the Im−[Co^{III}corrin]−Me^+ molecule and of the corresponding Im−[Co^{II}corrin]$^+$ and Me dissociation fragments. The performance of 19 representative DFT approaches, including a variety of GGA (OLYP, BLYP, TPSS, MPWPW91, M06-L, BP86) and hybrid (BHandHLYP, MPW1K, M06-2X, MPW1PW91, B3LYP, M06, TPSSh) functionals, augmented with the dispersion-corrected BP86+D2, BP86+D3, B97-D, B3LYP+D2, B3LYP+D3, and ωB97X-D data, along with the corresponding CR-CC(2,3)/CCSD reference BDE values discussed in section 3.1, are summarized in Table 3 and Figure 8. For each of the two basis sets used in the present study, the BDEs resulting from the various DFT calculations, corrected for the ZPE and BSSE contributions, span a very wide range of values, between 1.2 and 40.4 kcal/mol when the 6-31G* basis set is employed and between −2.2 and 41.1 kcal/mol when the 6-311++G** basis set is utilized. Both ranges are way outside the experimental range of 32−40 kcal/mol, and it is also apparent that very few functionals are capable of producing BDE values that would match the reference CR-CC(2,3)/CCSD estimates, even when the larger, 6-311++G** basis set is employed. As mentioned earlier, the ZPE values obtained with different functionals are almost identical (to within ∼1 kcal/mol), with the average ZPE resulting from the various DFT calculations performed in this work being 5.3 kcal/mol. Thus, the wide range of BDE values resulting from various DFT calculations cannot be caused by

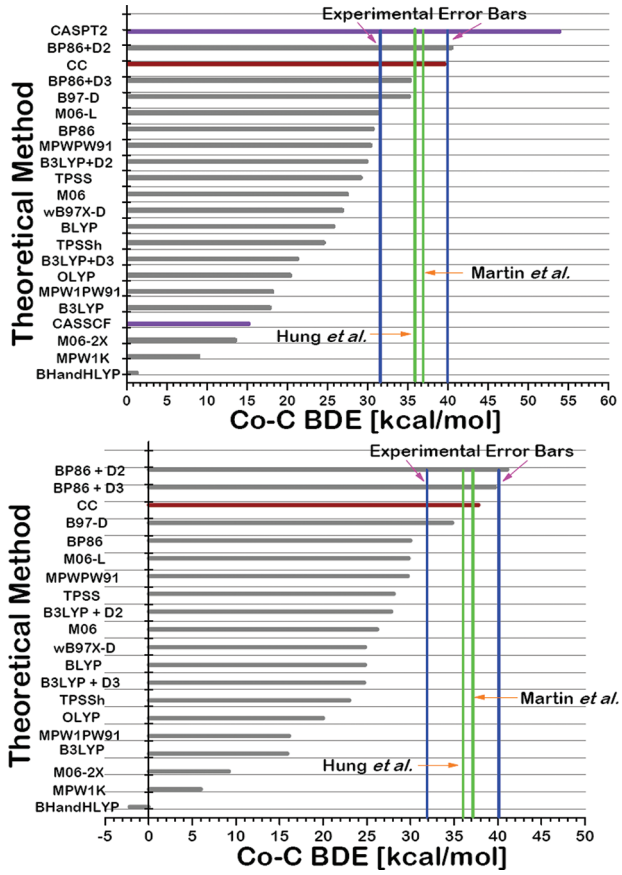

Figure 8. A comparison of the ZPE- and BSSE-corrected BDE values characterizing the Co−C_{Me} bond in the Im−[Co^{III}corrin]−Me^+ system resulting from various DFT calculations (gray horizontal bars) using the 6-31G* (top panel) and 6-311++G** (bottom panel) basis sets with the calculated (top panel) or extrapolated (bottom panel) ZPE-corrected CC [i.e., ζ = 0.003 CR-CC(2,3)/CCSD] BDE values (wine-colored horizontal bars) and their CASSCF(11,10) and CASPT2(11,10) counterparts [violet horizontal bars; the 6-31G*-like ANO-S basis set only]. In the case of the DFT approaches, the ZPE corrections were obtained with the 6-31G* basis set using the respective functionals. In the case of CR-CC(2,3)/CCSD, CASSCF(11,10), and CASPT2(11,10), the ZPE corrections were obtained in the BP86/6-31G* calculations, whereas the BSSE corrections, which are negligible in the local CC [including CR-CC(2,3)/CCSD] approaches and which are very large and, therefore, uncertain in the case of the CASSCF(11,10) and CASPT2(11,10) calculations using the 6-31G*-like ANO-S basis set when the counterpoise procedure is employed, were ignored (see the text for details). The vertical lines corresponding to the experimental BDE values reported in refs 22 and 23 are shown for comparison purposes.

the differences in the corresponding ZPE contributions. The optimized structural parameters of the Im−[Co^{III}corrin]−Me^+ system, including the axial Co−C_{Me} and Co−N_{Im} bond lengths listed in Table 3, do not seem to be the reason for the observed difficulties some DFT methods have with producing accurate BDE values either, since they show relatively small sensitivity with respect to the use of a particular functional. Indeed, in all cases, the optimized Co−C_{Me} distances characterizing the equilibrium geometry of Im−[Co^{III}corrin]−Me^+ agree reasonably well with the experimental (X-ray) value of 1.97 Å taken from ref 112. The agreement for the Co−N_{Im} distance is less satisfactory in a few cases (cf., e.g., the B3LYP, OLYP, and BLYP values), but the Co−N_{Im} bond lengths resulting from the

dx.doi.org/10.1021/ct300170y | J. Chem. Theory Comput. 2012, 8, 1870−1894

DFT calculations reported in Table 3 are, in most cases, accurate as well and in reasonable agreement with the X-ray value of 2.09 Å.[112] All of this implies that in trying to understand the wide range of BDE values resulting from various DFT calculations and in attempting to explain why only certain DFT methods provide reasonable BDEs that are consistent with experimental results and with the extrapolated, CR-CC(2,3)/6-311++G**-level, *ab initio* data, when so many other DFT approaches fail, one has to focus on the electronic contributions to the calculated BDEs.

As in other applications of DFT, the electronic component of each BDE is affected by both the one-electron basis set and the functional used in the calculations. It is clear, however, after examining the results collected in Table 3 and Figure 8, that the basis set used in the BDE calculations with DFT, although important, cannot be responsible for the observed variation in the DFT BDE values. This is reflected in the magnitudes of the BSSE contributions to the BDEs calculated with various DFT methods, which are in the 5.2−7.0 kcal/mol range when the 6-31G* basis set is employed and ∼1 kcal/mol when the 6-311++G** basis set is used (in agreement with the BSSE estimates reported in ref 98). None of these BSSE estimates are large enough to explain the enormous variation in the Co−C_{Me} dissociation energies obtained for the Im−[Co^{III}corrin]−Me^+ system with DFT. Moreover, after correcting the BDEs resulting from the DFT calculations for the BSSE effects, we obtain values that are in many cases almost insensitive to the basis set employed. Indeed, the differences between the BSSE-corrected BDE values obtained in the DFT calculations with the 6-31G* and 6-311++G** basis sets do not exceed 4.5 kcal/mol and are, in the majority of cases examined in Table 3 and Figure 8, in the ∼1−3 kcal/mol range (1.8 kcal/mol on average). Thus, in an effort to understand the enormous differences between the various DFT results, one has to focus on the ability of a given functional to capture the many-electron correlation effects involved in the breaking of the Co−C_{Me} bond in the Im−[Co^{III}corrin]−Me^+ molecule.

A closer inspection of the BDE data shown in Table 3 and Figure 8 reveals that, after correcting for the ZPE and BSSE contributions, only two of the 19 DFT approaches under consideration predict the Co−C_{Me} dissociation energies which fall into the experimental range of 32−40 kcal/mol. The two DFT methods that seem to work best, when compared to the experimental BDE data and our most accurate CR-CC(2,3)/CCSD/6-311++G**-level *ab initio* results, are B97-D and BP86+D3, with the B97-D functional, which produces a BDE of about 35 kcal/mol, performing particularly well. It should be noted that both B97-D and BP86+D3 belong to the category of pure, GGA-type, functionals corrected for dispersion interactions via the semiempirical "+D" corrections. As shown in Table 3 and Figure 8, and as elaborated on below, the analogous attempts to correct hybrid functionals, such as the popular B3LYP approach, are not nearly as effective once the larger basis set of 6-311++G** quality is used and the BSSE effects are accounted for. Of all functionals analyzed in this work, B97-D is the only one that provides the BDE within the 35−38 kcal/mol range established on the basis of the CR-CC(2,3)-level data and the intrinsic errors that may characterize them, as detailed in section 3.1. The hybrid ωB97X-D analog of B97-D works much worse than the B97-D functional, in spite of the presence of dispersion corrections in both functionals. On the basis of the results collected in Table 3 and Figure 8, it is quite clear that it is difficult to obtain a proper description of the Co−C_{Me} bond dissociation in MeCbl based on the DFT calculations exploiting hybrid functionals. There is a rather significant gap between the BDEs obtained with the GGA functionals, particularly those resulting from the TPSS, MPWPW91, M06-L, and BP86 calculations, which give BDEs in the ∼28−30 kcal/mol range, and those obtained with the hybrid functionals, which give (much) lower BDE values. As pointed out in ref 97, this gap persists when both types of functionals are corrected for dispersion interactions.

In general, most DFT functionals produce BDE values that are below the theoretical lower bound of about 35 kcal/mol, estimated on the basis of the CR-CC(2,3)-level calculations discussed in section 3.1 that suggest that the BDE of the isolated Im−[Co^{III}corrin]−Me^+ system is, most likely, in the 35−38 kcal/mol range. In fact, the vast majority of the DFT functionals benchmarked in this study produce BDEs below 32 kcal/mol, which is the experimentally determined lower bound, and the significant underestimation of the BDE values is mainly observed in those DFT calculations that rely on the hybrid functionals with a substantial amount of the exact HF exchange. The magnitude of the error in the BDE values resulting from the use of hybrid DFT approaches is approximately proportional to the percentage of the HF exchange in the corresponding functional. Two examples illustrate this statement best, namely the BLYP/B3LYP pair, where we obtain ∼25−26 kcal/mol in the BLYP case and ∼16−18 kcal/mol in the case of B3LYP, and the TPSS/TPSSh pair, where TPSS gives ∼28−29 kcal/mol and TPSSh, ∼23−25 kcal/mol. The BDE value of 24.8 kcal/mol obtained with the pure BLYP functional that contains 0% HF exchange, using the 6-311++G** basis set, is much closer to the experimental and extrapolated CR-CC(2,3)/CCSD/6-311++G** reference data than the Co−C_{Me} dissociation energy of 15.9 kcal/mol resulting from the B3LYP/6-311++G** calculations, which incorporate a significant amount of the HF exchange (20%). A similar trend is observed when going from the TPSS functional that does not include the exact HF exchange, giving a BDE value of 28.1 kcal/mol when the 6-311++G** basis set is employed, to the hybrid TPSSh functional, which gives a less accurate result of 23.0 kcal/mol with the same basis, although the difference between the pure TPSS and hybrid TPSSh data is considerably (a factor of about 2) smaller than in the BLYP/B3LYP case, since the amount of HF exchange in TPSSh (10%) is much smaller (also by a factor of 2) than in the case of B3LYP. The DFT functionals that give the particularly low and poor Co−C_{Me} dissociation energies, in the 1.2−13.5 kcal/mol range when the 6-31G* basis set is used and in the −2.2 to +9.2 kcal/mol range when the 6-311++G** basis set is employed, namely, BHandHLYP, MPW1K, and M06-2X, contain ∼40−50% HF exchange, reinforcing our conclusions. All of these observations are in agreement with the results of the DFT calculations for the isomerization curves involving different structural motifs of the supported Cu_2O_2 cores, reported in refs 84 and 85, where the authors concluded that hybrid functionals tend to overstabilize diradical structures, producing incorrect relative energies, with the magnitude of error being proportional to the percentage of the HF exchange in the functional. In our view, the same rationale applies to the Co−C_{Me} bond dissociation in Im−[Co^{III}corrin]−Me^+, where the overstabilization of the increasingly diradical structures that emerge as the Co−C_{Me} bond is broken, relative to the equilibrium geometry, by the hybrid functionals with a significant amount of the HF exchange results in the BDE values which are much too low.

Table 5. A Comparison of the DFT and Reference CR-CC(2,3)/CCSD Energies at Selected Values of the Co−C_{Me} Distance in the Im−[Co^{III}corrin]−Me^+ System, R_{Co-C} (in Å), Obtained with the 6-31G* Basis Set, Relative to the Energy Values Obtained at the Equilibrium (R_{Co-C} = 1.969 Å) Geometry Resulting from the BP86/6-31G* Calculations[a]

R_{Co-C}	B3LYP	B3LYP+D2	B3LYP+D3	TPSS	MPWPW91	M06-L	BP86	BP86+D2	BP86+D3	B97-D	CR-CC(2,3)/CCSD[b]
1.969	0.00	0.00	0.00	0.00	0.00	0.00	0.00	0.00	0.00	0.00	0.00
2.00	0.24	0.31	0.25	0.16	0.14	0.25	0.13	0.20	0.12	0.04	0.53
2.40	15.72	17.18	16.00	14.52	13.91	15.71	13.82	15.42	14.14	13.47	15.02
2.80	22.00	27.79	25.22	29.79	30.15	30.00	30.24	33.98	31.35	29.06	29.80
3.20	26.83	32.58	29.87	35.52	36.69	33.48	37.16	42.46	40.13	35.56	38.31
3.60	27.87	35.46	32.33	37.51	38.93	36.49	39.59	46.56	44.25	39.37	42.35
4.00	28.08	37.10	34.02	38.51	40.06	38.98	40.77	48.58	46.51	41.69	44.23
4.50	28.63	37.17	34.35	38.69	40.22	40.66	40.88	48.52	46.63	43.30	44.85
MUE[c]	9.59	4.55	6.43	2.91	2.24	3.04	1.91	3.04	1.52	1.80	0.00
NPE[d]	16.92	9.84	11.48	6.16	4.98	6.55	4.41	4.68	3.16	2.98	0.00

[a]All energies are in kcal/mol. [b]Results of the CR-CC(2,3)/CCSD calculations with ζ = 0.003. [c]Mean unsigned error relative to CR-CC(2,3)/CCSD using the results obtained at R_{Co-C} = 2.0, 2.4, 2.8, 3.2, 3.6, 4.0, and 4.5 Å. [d]Nonparallelity error relative to CR-CC(2,3)/CCSD using the results obtained at R_{Co-C} = 2.0, 2.4, 2.8, 3.2, 3.6, 4.0, and 4.5 Å.

We believe that it is the excessive lowering of the electronic energies of the Im−[Co^{III}corrin]−Me^+ system at larger Co−C_{Me} separations rather than the neglect of dispersion interactions at shorter Co−C_{Me} distances which is the main reason for the substantial underestimation of the Co−C_{Me} dissociation energy by B3LYP (and other hybrid approaches with the significant fraction of the HF exchange), observed in refs 94 and 95, and confirmed in the present study.

At the same time, it is also true that one cannot obtain the BDE values within the experimental range of 32−40 kcal/mol, not to mention the projected theoretical range of about 35−38 kcal/mol corresponding to the CR-CC(2,3)-level calculations discussed in section 3.1, without dispersion corrections to the DFT energies using the functionals exploited in the present study, particularly when the larger basis set is employed and the BSSE contributions are accounted for [as pointed out in section 2.3, one does not have to worry about the BSSE effects when the local correlation CIM-CC methodology, exploited in this study to obtain the CR-CC(2,3)-level information, is utilized]. The pure GGA functionals, such as, e.g., BP86, give BDEs that are much closer to the experimental and our best *ab initio*, CR-CC(2,3)-level, estimates than those obtained with the hybrid functionals, but one has to include dispersion corrections to bring the results obtained with the GGA functionals to a reasonable agreement with the experimentally derived or CR-CC(2,3)-level data. Having said this, it is also important to re-emphasize that the analogous dispersion corrections added to the hybrid functionals do not suffice once the basis set is large enough and the BSSE effects are taken into account. This can be seen by comparing the ωB97X-D/6-311++G** BDE value of 24.8 kcal/mol with the much better B97-D/6-311++G** result of 34.8 kcal/mol. Both methods use the "+D2" corrections, and yet the results are dramatically different. They are so different, since ωB97X-D has a significant (22%) amount of the HF exchange which is not present in B97-D. One can see the same behavior by comparing the B3LYP and B3LYP+D2 or B3LYP+D3 results, where the use of the "+D" corrections helps the B3LYP calculations, increasing the corresponding BDE values by about 10 kcal/mol, bringing them closer to the experimental and CR-CC(2,3)-level-based ranges of 32−40 and 35−38 kcal/mol, respectively, but the B3LYP+D2 and B3LYP+D3 BDE values, after correcting for the ZPE and BSSE contributions, of 27.8 and 24.7 kcal/mol, respectively, when the 6-311++G** basis set is employed, are still too low.

Let us finally turn to the comparison of the Co−C_{Me} bond breaking curves, resulting from the selected DFT calculations, including the pure (TPSS, MPWPW91, M06-L, BP86) and dispersion-corrected (BP86+D2, BP86+D3, B97-D) GGA functionals, and their hybrid (B3LYP, B3LYP+D2, B3LYP+D3) counterparts, with the reference curve obtained in our best CR-CC(2,3)/CCSD calculations using ζ = 0.003, shown in Figure 6 and Table 5. As explained earlier, all of these curves were obtained by performing the single-point DFT and CC energy calculations using the 6-31G* basis set at the selected points along the one-dimensional PES cut obtained in the constrained BP86/6-31G* geometry optimizations. To provide numerical characteristics of each DFT curve examined in Figure 6 and Table 5, we computed the corresponding MUE and NPE values relative to the CR-CC(2,3)/CCSD reference data (cf. Table 5). Clearly, the use of the relatively small 6-31G* basis set to generate the DFT and CR-CC(2,3)/CCSD electronic energies means that our analysis of the resulting bond breaking curves has a largely qualitative character. On the other hand, one obtains interesting insights into the performance of DFT methods by examining the dissociation curves shown in Figure 6 and Table 5.

Indeed, the hybrid B3LYP functional provides an erratic dissociation curve, which splits from the benchmark CR-CC(2,3)/CCSD curve already at the small stretches of the Co−C_{Me} bond, resulting in the substantial and unphysical lowering of the B3LYP energies at larger Co−C_{Me} separations. Although one would have to use larger basis sets in the CR-CC(2,3)/CCSD and DFT calculations, and correct the DFT potential energy curves shown in Figure 6 and Table 5 for the BSSE effects to offer a more quantitative analysis (we have not done it, since the determination of BSSE at shorter Co−C_{Me} distances cannot be done as precisely as desired), it is quite clear that the MUE and NPE values relative to the benchmark CR-CC(2,3)/CCSD/6-31G* calculations of almost 10 and 17 kcal/mol, respectively, characterizing the raw B3LYP/6-31G* dissociation curve, and the ∼16 kcal/mol differences between the B3LYP and CR-CC(2,3)/CCSD energies obtained with the 6-31G* basis set at larger Co−C_{Me} distances are too large to produce a reasonable description of the Co−C_{Me} bond breaking in the Im−[Co^{III}corrin]−Me^+ molecule with the B3LYP functional. On the basis of the information in Table 3,

the use of basis sets larger than 6-31G* and the incorporation of BSSE effects make the situation only worse, lowering the BSSE-uncorrected B3LYP/6-31G* curve in the asymptotic region even more, by at least ∼8 kcal/mol. According to the error analysis presented in section 3.1, the CR-CC(2,3)/CCSD dissociation curve will lower too, when the larger basis set is employed, but the amount of this lowering, even when we account for the intrinsic errors of the local correlation CR-CC(2,3)/CCSD and canonical CR-CC(2,3) calculations, which is on the order of a few kilocalories per mole, is certainly not enough to bring the B3LYP and CR-CC(2,3)/CCSD curves to a better agreement compared to the results obtained with the 6-31G* basis set. According to Tables 3 and 5, and as shown in Figure 6b, by increasing the binding energy characterizing the Im−[Co^{III}corrin]−Me$^+$ system, the dispersion "+D" corrections move the B3LYP asymptote up, toward the CR-CC(2,3)/CCSD curve, reducing the large MUE and NPE values characterizing the B3LYP calculations from about 10 and 17 kcal/mol to 5−6 and 10−11 kcal/mol, respectively, but again this is not enough to compensate for the substantial differences between the B3LYP and CR-CC(2,3)/CCSD energies at larger Co−C$_{Me}$ separations observed in Figure 6a and Table 5, particularly when the basis set and BSSE effects are accounted for. It is, therefore, the significant overstabilization of the increasingly diradical structures that emerge as the Co−C$_{Me}$ bond is broken by the B3LYP functional, resulting in the erratic dissociation curves, shown in Figure 6a for the bare B3LYP approach and in Figure 6b for the B3LYP+D2 and B3LYP+D3 methods, which is the primary reason why this functional, even after correcting for dispersion interactions, cannot produce accurate BDE values. Similar remarks apply to other hybrid functionals with a significant amount of the HF exchange, which all underestimate the Co−C$_{Me}$ BDE in Im−[Co^{III}corrin]−Me$^+$.

It is clear from Figure 6a and Table 5 that the potential energy curves resulting from the use of the GGA functionals (represented in Figure 6a and Table 5 by the TPSS, MPWPW91, M06-L, and BP86 approaches) provide a substantial improvement over the results of the B3LYP calculations, reducing the large MUE and NPE values relative to the benchmark CR-CC(2,3)/CCSD/6-31G* data characterizing the raw B3LYP/6-31G* dissociation curve, of ∼10 and ∼17 kcal/mol, to ∼2−3 and ∼4−7 kcal/mol, respectively. The inclusion of dispersion corrections, illustrated in Figure 6b and Table 5 by the results obtained with the BP86+D2, BP86+D3, and B97-D functionals, may offer additional improvements, which are particularly impressive in the case of the B97-D calculations that give the MUE and NPE values of less than 2 and 3 kcal/mol, respectively. Although we cannot produce direct evidence for this, since the large-basis-set CR-CC(2,3)/CCSD calculations with the suitably small ζ values, such as ζ = 0.003, needed to obtain an accurate description of the Co−C$_{Me}$ bond breaking in the Im−[Co^{III}corrin]−Me$^+$ system, are prohibitively expensive, we can argue, on the basis of the estimated basis set dependence and the error analysis characterizing the CR-CC(2,3)-level calculations presented in section 3.1, that the description of the Co−C$_{Me}$ bond dissociation by the B97-D functional and the resulting BDE values are of very high quality, with BP86+D3 performing very well, too. Indeed, according to the considerations presented in section 3.1, we expect the CR-CC(2,3)/CCSD/6-31G* reference curve obtained with ζ = 0.003 to lower by about 2 kcal/mol in the asymptotic region and by up to about 4 kcal/mol in the region of the intermediate Co−C$_{Me}$ separations around 3.0 Å, when the larger 6-311++G** basis set is employed (assuming that we continue using the energy scale in which the equilibrium geometry corresponds to 0 kcal/mol for each theory level). We expect an additional ∼2−3 kcal/mol lowering of the resulting CR-CC(2,3)/6-311++G**-quality curve at larger Co−C$_{Me}$ distances when approaching convergence with respect to the many-electron correlation effects and basis set. Thus, the extrapolated and reasonably well converged nonrelativistic *ab initio* curve is expected to be lower than the CR-CC(2,3)/CCSD/6-31G* curve shown in Figure 6 and Table 5 by up to about 6−7 kcal/mol in the region of the intermediate Co−C$_{Me}$ separations and by about 4−5 kcal/mol in the asymptotic region. On the basis of the results in Tables 3 and 5, the B97-D curve converged with respect to the basis set is expected to be very similar, to within ∼2−3 kcal/mol, in terms of the relative energetics (the MUE and NPE values) and the overall shape, to the converged form of the *ab initio* curve, as described above. Indeed, the difference between the purely electronic BDE resulting from the raw, BSSE-uncorrected, B97-D/6-31G* calculations that were used to produce the B97-D curve shown in Figure 6b and Table 5, of 46.3 kcal/mol [cf. the sum of the ZPE, BSSE, and BDE contributions listed in columns 4−6 of Table 3] and its BSSE-corrected B97-D/6-311++G** counterpart, estimated at 40.1 kcal/mol [cf. the sum of the ZPE and BDE contributions listed in columns 4 and 8 of Table 3], is ∼6 kcal/mol, i.e., one can expect a similar amount of lowering of the B97-D curve shown in Figure 6b and Table 5 at larger Co−C$_{Me}$ distances as that expected in the CR-CC(2,3)/CCSD case. This reinforces our view about recommending the carefully optimized, dispersion-corrected, GGA functionals, such as B97-D, for studies of the Co−C dissociation in MeCbl and other cobalamins. Our calculations indicate that the B97-D functional describes the Co−C$_{Me}$ dissociation in the isolated Im−[Co^{III}corrin]−Me$^+$ molecule at the level matching the most accurate CC calculations, so that building computational models of cobalamins based on the B97-D functional, which should ultimately include solvation, thermal, and other physical effects that we neglected in this work, seems reasonable. On the basis of the results in Tables 3 and 5, and Figures 6 and 8, other dispersion-corrected GGA-type functionals, such as BP86+D3, can be recommended for accurate modeling of the Co−C dissociation in cobalamins, too. We cannot, however, recommend, hybrid functionals, such as B3LYP, even when corrected for dispersion interactions via the "+D" corrections, since the resulting BDEs are underestimated too much.

3.3. Comparison with CASSCF and CASPT2 Calculations. To enrich our discussion, we also determined the Co−C$_{Me}$ BDEs and the corresponding dissociation curves using the CASSCF(11,10) and CASPT2(11,10) calculations, as described in section 2.4. The purely electronic BDE values obtained by performing single-point calculations at the BP86/6-31G* optimized geometries of the Im−[Co^{III}corrin]−Me$^+$ molecule and of the corresponding Im−[Co^{II}corrin]$^+$ and Me dissociation radical fragments were found to be 20.1 kcal/mol in the CASSCF(11,10) case and 58.8 kcal/mol in the case of CASPT2(11,10). None of these estimates are in harmony with the reference CR-CC(2,3)/CCSD and experimental BDE values. Upon inclusion of the ZPE corrections resulting from the BP86/6-31G* calculations, the Co−C$_{Me}$ dissociation energy predicted by CASSCF(11,10) remains too low (15.1 kcal/mol), while the CASPT2(11,10) BDE value is still too high (53.8 kcal/mol; see Figure 8). The difficulty the

CASSCF(11,10) and CASPT2(11,10) calculations have with producing reasonable BDE values must be related to the substantial differences between the Co−C_{Me} bond dissociation curves resulting from the CASSCF(11,10) and CASPT2(11,10) calculations, shown in Figure 7, and the analogous curve obtained in the benchmark CR-CC(2,3)/CCSD calculations, shown in Figure 6.

The disagreement between the CASSCF(11,10) and experimental or CR-CC(2,3)/CCSD BDE values and the CASSCF(11,10) and CR-CC(2,3)/CCSD dissociation curves can certainly be attributed to the neglect of dynamical correlation effects in the CASSCF calculations. These effects are particularly important around the equilibrium geometry, and their neglect produces electronic energies that often are, in absolute value, too small when compared to the asymptotic region, resulting in the underestimated BDE value. The disagreement between the CASPT2(11,10) and experimental or CR-CC(2,3)/CCSD BDE values and the reasons for the substantial differences between the CASPT2(11,10) and CR-CC(2,3)/CCSD dissociation curves obtained with similar basis sets are less transparent, since CASPT2 includes the non-dynamical as well as dynamical correlations, but not entirely surprising either. Indeed, in order for CASPT2 to work, one has to make sure that the active space used in the CASSCF and subsequent CASPT2 calculations is large enough for the problem of interest. The huge, 38.7 kcal/mol, difference between the BDE values characterizing the Co−C_{Me} bond in Im−[Co^{III}corrin]−Me^+ and resulting from the CASSCF and CASPT2 calculations employing the same (11,10) active space, and the analogously large difference between the CASSCF(11,10) and CASPT2(11,10) dissociation curves shown in Figure 7 indicate the excessive second-order energy correction that tries to compensate for the deficiencies of the CASSCF(11,10) reference wave function but cannot completely eliminate them. The orbital delocalization involving the in-plane nitrogen and carbon atoms around Co and the rapidly growing significance of the single and double excitations to the unoccupied orbitals mixing the Co−C_{Me} antibonding $\sigma^*(d_{z^2})$ character with the delocalized network of orbitals that reflects on the corrin conjugation around the cobalt center as the Co−C_{Me} bond is stretched, observed in the canonical and local CC calculations discussed in section 3.1, point to the inadequacy of the (11,10) active space as well. Due to prohibitive computer costs of CASSCF calculations employing larger active spaces, the active orbitals used in our CASSCF(11,10) calculations had to be largely centered on the axial fragment comprised of Co and C_{Me} atoms, so that a lot of information about the excitations to the unoccupied orbitals mixing the antibonding $\sigma^*(d_{z^2})$ character with the delocalized network of orbitals reflecting on the corrin conjugation around Co had to be neglected. On the basis of the analysis of the canonical and local CC wave functions in section 3.1, the presence of these additional excitations that couple the substantial nondynamical and dynamical correlation effects at larger Co−C_{Me} separations, combined with the relatively large single excitations of the $\sigma(d_{z^2})\rightarrow\sigma^*(d_{z^2})$ type, in addition to the equally important double $\sigma(d_{z^2})\rightarrow\sigma^*(d_{z^2})$ excitations, which, as shown in Figure 7, do not show up in the CASSCF(11,10) wave functions in the $R_{Co-C} \approx 4.0-4.5$ Å region where the CR-CC(2,3)/CCSD reference curve already levels off, is essential to stabilize the Co−C_{Me} bond breaking curve around the energy values compatible with the experimental BDE data. The CASSCF(11,10) calculations do not capture these additional and, if we trust CC calculations, substantial effects, and the subsequent CASPT2 calculations based on the inadequate CASSCF(11,10) reference have difficulties with providing a balanced description of the dynamical and nondynamical correlation effects relevant to the Co−C_{Me} bond breaking in the Im−[Co^{III}corrin]−Me^+ system.

In order to remedy the above situation, one would have to use a much larger active space, reflecting on the above remarks about the significance of the orbitals of the corrin conjugation around Co on the Co−C_{Me} dissociation process, but we were unable to include these additional orbitals in the CASSCF and CASPT2 calculations carried out in this study due to prohibitive computer costs. Being unable to increase the active space any further, we tested the importance of other factors that might help the CASSCF and CASPT2 results, including the role of scalar relativistic effects and BSSE. The computed relativistic effects, using the perturbation calculations of the one-electron Darwin contact term and also of the relativistic mass-velocity term[135] have an essentially negligible contribution (∼1.5 kcal/mol). On the other hand, the counterpoise BSSE corrections resulting from the CASSCF(11,10) and CASPT2(11,10) calculations, estimated at 6.7 and 19.7 kcal/mol, respectively, are substantial, lowering the corresponding Co−C_{Me} BDEs to 10.2 kcal/mol in the CASSCF(11,10) case and 35.9 kcal/mol in the case of the CASPT2(11,10) calculations. The latter result falls into the experimental range of 32−40 kcal/mol and is in good agreement with the CR-CC(2,3)/CCSD reference values shown in Table 3 and Figure 8, but the question arises to what extent the dissociation energy having such a large BSSE contribution, on the order of 50% of the experimental or CR-CC(2,3)/CCSD BDE values, can be trusted, particularly in the context of the covalent Co−C_{Me} bond dissociation and in a situation where the analogous correction obtained with CASSCF worsens the already poor CASSCF(11,10) BDE even further. There are several factors that might contribute to the large values of the BSSE corrections obtained with CASSCF(11,10) and CASPT2(11,10). One obvious reason is the relatively small size of the basis set used in the CASSCF(11,10) and CASPT2(11,10) calculations reported in this work, although this would seem to contradict our findings that the CR-CC(2,3)/CCSD and at least some DFT (e.g., B97-D) approaches using a similar basis set produce reasonable BDE values, which are a lot more consistent with experimental results and do not change much with the basis set, even in the case of the CC calculations that are known to converge more slowly with the basis set than the DFT results. On the other hand, as already pointed out, it is well established that the local correlation size extensive approaches, such as the local variant of the CR-CC(2,3) method employed in this study, efficiently eliminate BSSE, even when the relatively small basis sets are employed,[131] which the conventional CASPT2 calculations cannot do. This could be another reason why the CR-CC(2,3)/CCSD/6-31G* results for the Co−C_{Me} bond dissociation in Im−[Co^{III}corrin]−Me^+ are already quite good, in spite of the use of the relatively small basis set, when the analogous CASPT2(11,10)/ANO-S results neglecting BSSE are rather poor. Another factor that might contribute to some of the inaccuracies observed in our CASPT2(11,10) calculations is the size inextensivity of the "diagonalize-then-perturb" CASPT2 approach used in this work,[136] which may become a problem in calculations for large systems of the type of the Im−[Co^{III}corrin]−Me^+ model of MeCbl examined in this work,

but it is hard to prove this. The CR-CC(2,3) approach and its multilevel CR-CC(2,3)/CCSD extension mixing local CR-CC(2,3) with canonical CCSD are size extensive, so we do not expect a loss of accuracy in CR-CC(2,3)-level calculations only because the molecular system of interest becomes larger. Nevertheless, we believe that the counterpoise correction of about 20 kcal/mol characterizing our CASPT2(11,10) calculations for the Im−[Co^{III}corrin]−Me^+ system is too large to be treated as an accurate estimate of the BSSE contribution to the Co−C_{Me} BDE; i.e., the counterpoise- and ZPE-corrected CASPT2(11,10) BDE of 35.9 kcal/mol may be a result of the fortuitous cancellation of errors, although this has to be analyzed further, in conjunction with the examination of larger and more appropriate basis sets and active spaces that reflect on the nature of the dominant excitation amplitudes in CC wave functions.

Our plan is to use one of the incomplete model-space multireference perturbation theory models that should allow us to include larger numbers of active orbitals and basis functions in the calculations. We will also examine the performance of the CASSCF and CASPT2 approaches in the calculations for smaller problems, such as the $Co(NH_3)_5(Me)^{2+}$ complex used in this work, although we must keep in mind that the active space appropriate for describing the Co−C_{Me} dissociation in the $Co(NH_3)_5(Me)^{2+}$ molecule may not be transferrable to the much larger Im−[Co^{III}corrin]−Me^+ system.

4. SUMMARY AND CONCLUSIONS

The Co−C_{Me} bond dissociation in the MeCbl cofactor, modeled by the Im−[Co^{III}corrin]−Me^+ system consisting of 58 atoms, was examined using a variety of CC and DFT methods and the CASSCF and CASPT2 approaches. The suitably designed and carefully validated multilevel variant of the local correlation CIM framework, employing the triples corrections of the CR-CC(2,3) theory to describe higher-order many-electron correlation effects in the chemically active region, where the Co−C_{Me} bond breaking takes place, and the canonical CCSD approach to describe the remaining correlation effects in the chemically active and inactive regions, abbreviated as CR-CC(2,3)/CCSD, was used to obtain the benchmark, CR-CC(2,3)-level, *ab initio* potential energy curve and information about the dissociation energy range characterizing the Co−C_{Me} bond breaking in the MeCbl species. The Co−C_{Me} dissociation energy resulting from the CR-CC(2,3)/CCSD calculations for the Im−[Co^{III}corrin]−Me^+ system, corrected for the ZPEs obtained with DFT, is about 40 kcal/mol, when the 6-31G* basis set is employed, with the estimated error relative to the corresponding canonical CR-CC(2,3)/6-31G* result on the order of less than 1 kcal/mol. The extrapolated CR-CC(2,3)/CCSD result corresponding to the larger 6-311++G** basis set, obtained by combining the ZPE-corrected CR-CC(2,3)/CCSD energies obtained using the 6-31G* basis set with the results of the auxiliary canonical CR-CC(2,3)/6-31G* and CR-CC(2,3)/6-311++G** calculations for the $Co(NH_3)_5(Me)^{2+}$ model complex in its lowest-energy singlet state, is about 38 kcal/mol, in excellent agreement with the available experimental BDE values characterizing the MeCbl cofactor of 37 ± 3 and 36 ± 4 kcal/mol.[22,23] On the basis of what is known about the performance of the CR-CC(2,3) approach in single bond breaking situations and the analysis of the potential sources of errors in the local and canonical CR-CC(2,3)-level calculations performed in this work, it is anticipated that the ZPE-corrected Co−C_{Me} dissociation energy characterizing the isolated Im−[Co^{III}corrin]−Me^+ system is in the 35−38 kcal/mol range, which is consistent with the experimental range (including error bars) of 32−40 kcal/mol characterizing the MeCbl cofactor. This, in turn, implies that the solvation and thermal effects, which contribute to the experimentally determined dissociation energies, but were not considered in the calculations for the Im−[Co^{III}corrin]−Me^+ system reported in this work, cannot play a major role, in agreement with the earlier studies (cf., e.g., refs 97 and 98). More importantly, the DFT and DFT+D methods (and other quantum chemistry approaches), which produce BDE values that are considerably outside the 35−38 kcal/mol range, when the isolated Im−[Co^{III}corrin]−Me^+ system is examined, should not be recommended for calculations for cobalamins or used with caution.

The Co−C_{Me} dissociation energies and curve resulting from the CR-CC(2,3)/CCSD reference calculations and the experimental dissociation energy values were used to assess the accuracy of various DFT and CASSCF/CASPT2 methods. We demonstrated that of the 19 DFT approaches examined in the present study, the best dissociation energies and the overall most accurate description of the Co−C_{Me} bond breaking in the Im−[Co^{III}corrin]−Me^+ system are provided by the B97-D approach, which gives a BDE value of about 35 kcal/mol, when the 6-311++G** basis set is employed and when the results are corrected for the ZPE and BSSE contributions, in very good agreement with experimental results and the CR-CC(2,3)/CCSD reference data. With the exception of the B97-D and BP86+D3 approaches, none of the other DFT methods examined in the present study produces results that fall into the experimental range of the Co−C_{Me} dissociation energies in MeCbl of 32−40 kcal/mol.

We provided convincing evidence that the DFT approaches that rely on the hybrid functionals with the substantial amount of the exact HF exchange, such as, for example, B3LYP, considerably underestimate the calculated dissociation energies, with the magnitude of the error being proportional to the percentage of the HF exchange in the functional, in agreement with the observations made in refs 84 and 85 in which the authors concluded that hybrid density functionals tend to overstabilize diradical structures, producing incorrect relative energies. On the basis of a large number of DFT calculations using two different basis sets, hybrid as well as GGA functionals with and without dispersion corrections, and comparisons with the available experimental and benchmark, CR-CC(2,3)-level, *ab initio* data, we demonstrated that it is the overstabilization of the increasingly diradical structures that emerge as the Co−C_{Me} bond is broken by the hybrid functionals with a significant amount of the HF exchange rather than the neglect of dispersion interactions at shorter Co−C_{Me} distances, postulated in some other recent studies,[94,95] which is the primary reason for the substantial underestimation of the Co−C_{Me} dissociation energy by the B3LYP and other hybrid functionals, particularly when the larger 6-311++G** basis set is employed and BSSE is accounted for. At the same time, we provided evidence that one cannot obtain the BDE values within the experimental range of 32−40 kcal/mol, not to mention the projected theoretical range of about 35−38 kcal/mol extracted from the CR-CC(2,3)-level calculations reported in this work, without dispersion corrections to the DFT energies when the basis set is larger and the effects of BSSE are taken into consideration. The results reported in the present work

indicate that the most reasonable approach to the accurate modeling of the Co−C dissociation in MeCbl and other cobalamins is to use one of the carefully optimized, dispersion-corrected, GGA functionals, such as the B97-D approach, which is capable of providing the Co−C_{Me} dissociation curve and the Co−C_{Me} dissociation energy within the error bars of the high-accuracy, CR-CC(2,3)-level, *ab initio* data and within the error bars characterizing the experimental BDE values. Other dispersion-corrected GGA-type functionals, such as, for example, BP86+D3, can be recommended, too. We cannot, however, recommend, hybrid functionals, such as B3LYP, even when corrected for dispersion interactions via the "+D" corrections, when the Co−C dissociation in MeCbl and other cobalamins is to be examined, since the resulting BDEs can be significantly underestimated once the larger basis set is employed and BSSE is accounted for. On the other hand, most of the functionals examined in the present study, including pure as well as hybrid schemes, provide an accurate description of the key structural parameters of MeCbl, such as the axial C−C_{Me} and C−N_{Im} bond lengths, which are in good agreement with the available X-ray data.

In addition to reporting the variety of DFT and the benchmark CR-CC(2,3)-type results, the problem of Co−C_{Me} cleavage in MeCbl was investigated using the CASSCF and CASPT2 approaches, which are often recommended as the methods of choice for studies involving bond breaking. We demonstrated that the CASSCF and CASPT2 methods have difficulties with providing a reliable description of the Co−C_{Me} bond breaking in the Im−[Co^{III}corrin]−Me^+ model of MeCbl that would be consistent with the experimental BDEs and the carefully calibrated CR-CC(2,3)/CCSD-level data, since using adequate active spaces is prohibitively expensive, whereas smaller and affordable active spaces are insufficient for carrying out meaningful calculations. On the basis of the analysis of the CC wave functions, we concluded that the presence of the excited configurations which involve the unoccupied orbitals mixing the Co−C_{Me} antibonding $\sigma^*(d_{z^2})$ character with the delocalized network of orbitals reflecting on the corrin conjugation around the Co center and which couple the substantial nondynamical and dynamical correlation effects at larger Co−C_{Me} separations, combined with the large single and double excitations of the axial $\sigma(d_{z^2})\rightarrow\sigma^*(d_{z^2})$ type, are essential to stabilize the Co−C_{Me} bond breaking curve around the energy values compatible with the experimental dissociation energy data. Unfortunately, due to prohibitive computer costs of CASSCF and CASPT2 calculations employing larger active spaces, the active orbitals used in our CASSCF and CASPT2 calculations had to be largely centered on the axial fragment comprised of Co and C_{Me} atoms, so that a lot of information about the excitations to the unoccupied orbitals mixing the antibonding $\sigma^*(d_{z^2})$ character with the delocalized network of orbitals reflecting on the corrin conjugation around Co had to be neglected.

■ ASSOCIATED CONTENT

Supporting Information

The BP86/6-31G*-optimized structure of the Im−[Co^{III}corrin]−Me^+ system (a Co−C_{Me} distance of 1.969 Å), the geometries of Im−[Co^{III}corrin]−Me^+ along the Co−C_{Me} bond breaking coordinate resulting from the constrained BP86/6-31G* optimizations corresponding to the Co−C_{Me} distances of 2.0, 2.4, 2.8, 3.2, 3.6, 4.0, and 4.5 Å, the BP86/6-31G*-optimized structure of the $Co(NH_3)_5(Me)^{2+}$ model complex (a Co−C_{Me} distance of 1.9575 Å), and the geometries of $Co(NH_3)_5(Me)^{2+}$ along the Co−C_{Me} bond breaking coordinate obtained in the constrained BP86/6-31G* optimizations corresponding to the Co−C_{Me} distances of 2.2, 2.4, 2.6, 2.8, 3.0, 3.5, 4.0, and 4.5 Å. This material is available free of charge via the Internet at http://pubs.acs.org.

■ AUTHOR INFORMATION

Corresponding Author

*E-mail: pawel@louisville.edu (P.M.K.) and piecuch@chemistry.msu.edu (P.P.).

Notes

The authors declare no competing financial interest.

■ ACKNOWLEDGMENTS

This work has been supported by the U.S. Department of Energy (Grant No. DE-FG02-01ER15228; P.P.), the Spectral Sciences, Incorporated under the U.S. Air Force Contract No. FA9550-10-C-0093 (P.P.), and the Ministry of Science and Higher Education (Poland) under Grant No. N N204 028336. The MOLCAS 7.4 calculations were carried out at the Wrocław Centre for Networking and Supercomputing, Poland, under Grant No. 18/96. The TURBOMOLE V6.3 calculations were carried out at the Academic Computer Centre CYFRONET of the University of Science and Technology in Cracow, Poland, under grant Nos. MNiSW/SGI3700/UŚląski/111/2007 and MNiSW/IBM_BC_HS21/UŚląski/111/2007.

■ REFERENCES

(1) Dolphin, D. *B_{12}*; Wiley-Interscience: New York, 1982.
(2) Halpern, J. *Science* **1985**, *227*, 869.
(3) Banerjee, R. *Chem. Biol.* **1997**, *4*, 175.
(4) Ludwig, M. L.; Matthews, R. G. *Annu. Rev. Biochem.* **1997**, *66*, 269.
(5) *Vitamin B_{12} and B_{12} Proteins*; Kräutler, B., Arigoni, B., Golding, B. T., Eds.; Wiley-VCH: New York, 1998 (Lectures Presented at the 4th European Symposium on Vitamin B_{12} and B_{12} Proteins).
(6) Marzilli, L. G. In *Bioinorganic Catalysis*; Reedijk, J., Bouwman, E., Eds.; Marcel Dekker: New York, 1999; pp 423−468.
(7) Banerjee, R. *Chemistry and Biochemistry of B_{12}*; Wiley: New York, 1999.
(8) Toraya, T. *Cell. Mol. Life Sci.* **2000**, *57*, 106.
(9) Banerjee, R. *Biochemistry* **2001**, *40*, 6191.
(10) Matthews, R. G. *Acc. Chem. Res.* **2001**, *34*, 681.
(11) Banerjee, R.; Ragsdale, S. W. *Annu. Rev. Biochem.* **2003**, *72*, 209.
(12) Banerjee, R. *Chem. Rev.* **2003**, *103*, 2083.
(13) Toraya, T. *Chem. Rev.* **2003**, *103*, 2095.
(14) Brown, K. L. *Chem. Rev.* **2005**, *105*, 2075.
(15) Randaccio, L.; Geremia, S.; Nardin, G.; Wuerges, J. *Coord. Chem. Rev.* **2006**, *250*, 1332.
(16) Matthews, R. G.; Koutmos, M.; Datta, S. *Curr. Opin. Struct. Biol.* **2008**, *18*, 658.
(17) Randaccio, L.; Geremia, S.; Demitri, N.; Wuerges, J. *Trends Inorg. Chem.* **2009**, *11*, 1.
(18) Matthews, R. G. In *Metal Ions in Life Sciences*; Sigel, A., Sigel, H., Sigel, R. K. O., Eds.; Royal Society of Chemistry: Cambridge, U.K., 2009; Vol. *6*, pp 53−114.
(19) Randaccio, L.; Geremia, S.; Demitri, N.; Wuerges, J. *Molecules* **2010**, *15*, 3228.
(20) Finke, R. G. In *Vitamin B_{12} and B_{12} Proteins*; Krautler, B., Arigoni, D., Golding, B. T., Eds.; Wiley-VCH: Weinheim, Germany, 1998.
(21) Chowdhury, S.; Banerjee, R. *Biochemistry* **2000**, *39*, 7998.
(22) Martin, B. D.; Finke, R. G. *J. Am. Chem. Soc.* **1992**, *114*, 585.
(23) Hung, R. R.; Grabowski, J. J. *J. Am. Chem. Soc.* **1999**, *121*, 1359.

(24) Halpern, J.; Kim, S.-H.; Leung, T. W. *J. Am. Chem. Soc.* **1984**, *106*, 8317.
(25) Hay, B. P.; Finke, R. G. *Polyhedron* **1988**, *7*, 1469.
(26) (a) Chen, L. H.; Yan, H.; Luo, L.; Cui, X. X.; Tang, W. X. *J. Inorg. Chem.* **1997**, *66*, 219. (b) Luo, L. B.; Li, G.; Chen, H. L.; Fu, S. W.; Zhang, S. Y. *J. Chem. Soc., Dalton Trans.* **1998**, 2103. (c) Chen, H.; Li, G.; Shang, F. F.; Sun, L.; Chen., J. L.; Shang., S. Y. *Spectrochim. Acta, Part A* **2003**, *59*, 2767.
(27) Hollaway, M. R.; White, H. A.; Joblin, K. N.; Johnson, A. W.; Lappert, A. W.; Wallis, O. C. *Eur. J. Biochem.* **1978**, *82*, 143.
(28) Padmakumar, R.; Padmakumar, R.; Banerjee, R. *Biochemistry* **1998**, *37*, 11864.
(29) Marsh, E. N. G.; Ballou, D. P. *Biochemistry* **1998**, *37*, 11864.
(30) Licht, S. S.; Booker, S.; Stubbe, J. *Biochemistry* **1999**, *38*, 1221.
(31) (a) Hay, B. P.; Finke, R. G. *J. Am. Chem. Soc.* **1986**, *108*, 4820. (b) Hay, B. P.; Finke, R. G. *J. Am. Chem. Soc.* **1987**, *109*, 8012.
(32) (a) Laidig, W. D.; Purvis, G. D., III; Bartlett, R. J. *Int. J. Quantum Chem. Symp.* **1982**, *16*, 561. (b) Laidig, W. D.; Purvis, G. D., III; Bartlett, R. J. *Chem. Phys. Lett.* **1983**, *97*, 209. (c) Laidig, W. D.; Purvis, G. D., III; Bartlett, R. J. *J. Phys. Chem.* **1985**, *89*, 2161.
(33) (a) Förner, W.; Ladik, J.; Otto, P.; Čížek, J. *Chem. Phys.* **1985**, *97*, 251. (b) Förner, W. *Chem. Phys.* **1987**, *114*, 21.
(34) (a) Pulay, P. *Chem. Phys. Lett.* **1983**, *100*, 151. (b) Pulay, P.; Saebø, S. *Theor. Chim. Acta* **1986**, *69*, 357. (c) Saebø, S.; Pulay, P. *Chem. Phys. Lett.* **1985**, *113*, 13. (d) Saebø, S.; Pulay, P. *J. Chem. Phys.* **1987**, *86*, 914. (e) Saebø, S.; Pulay, P. *J. Chem. Phys.* **1988**, *88*, 1884. (f) Saebø, S.; Pulay, P. *Annu. Rev. Phys. Chem.* **1993**, *44*, 213.
(35) Takahashi, M.; Paldus, J. *Phys. Rev. B* **1985**, *31*, 5121.
(36) (a) Coester, F. *Nucl. Phys.* **1958**, *7*, 421. (b) Coester, F.; Kümmel, H. *Nucl. Phys.* **1960**, *17*, 477. (c) Čížek, J. *J. Chem. Phys.* **1966**, *45*, 4256. (d) Čížek, J. *Adv. Chem. Phys.* **1969**, *14*, 35. (e) Čížek, J.; Paldus, J. *Int. J. Quantum Chem.* **1971**, *5*, 359.
(37) Bartlett, R. J.; Musiał, M. *Rev. Mod. Phys.* **2007**, *79*, 291 and references therein.
(38) (a) Ye, Y.-J.; Förner, W.; Ladik, J. *Chem. Phys.* **1993**, *178*, 1. (b) Knab, R.; Förner, W.; Čížek, J.; Ladik, J. *THEOCHEM* **1996**, *366*, 11. (c) Förner, W.; Knab, R.; Čížek, J.; Ladik, J. *J. Chem. Phys.* **1997**, *106*, 10248.
(39) Scuseria, G. E.; Ayala, P. Y. *J. Chem. Phys.* **1999**, *111*, 8330.
(40) (a) Hampel, C.; Werner, H.-J. *J. Chem. Phys.* **1996**, *104*, 6286. (b) Schütz, M.; Werner, H.-J. *J. Chem. Phys.* **2001**, *114*, 661. (c) Schütz, M. *J. Chem. Phys.* **2000**, *113*, 9986. (d) Schütz, M.; Werner, H.-J. *Chem. Phys. Lett.* **2000**, *318*, 370. (e) Schütz, M. *J. Chem. Phys.* **2002**, *116*, 8772. (f) Schütz, M. *Phys. Chem. Chem. Phys.* **2002**, *4*, 3941. (g) Schütz, M.; Rauhut, G.; Werner, H.-J. *J. Phys. Chem. A* **1998**, *102*, 5997. (h) Mata, R. A.; Werner, H.-J. *J. Chem. Phys.* **2006**, *125*, 184110. (i) Adler, T. B.; Knizia, G.; Werner, H.-J. *J. Chem. Phys.* **2009**, *130*, 241101.
(41) (a) Korona, T.; Werner, H.-J. *J. Chem. Phys.* **2003**, *118*, 3006. (b) Korona, T.; Pflüger, K.; Werner, H.-J. *Phys. Chem. Chem. Phys.* **2004**, *6*, 2059. (c) Kats, D.; Korona, T.; Schütz, M. *J. Chem. Phys.* **2006**, *125*, 104106. (d) Kats, D.; Korona, T.; Schütz, M. *J. Chem. Phys.* **2007**, *127*, 064107.
(42) Maslen, P. E.; Lee, M. S.; Head-Gordon, M. *Chem. Phys. Lett.* **2000**, *319*, 205.
(43) (a) Subotnik, J. E.; Head-Gordon, M. *J. Chem. Phys.* **2005**, *123*, 064108. (b) Subotnik, J. E.; Sodt, A.; Head-Gordon, M. *J. Chem. Phys.* **2006**, *125*, 074116. (c) Subotnik, J. E.; Sodt, A.; Head-Gordon, M. *J. Chem. Phys.* **2008**, *128*, 034103.
(44) (a) Russ, N. J.; Crawford, T. D. *J. Chem. Phys.* **2004**, *121*, 691. (b) Crawford, T. D.; King, R. A. *Chem. Phys. Lett.* **2002**, *366*, 611. (c) Russ, N. J.; Crawford, T. D. *Phys. Chem. Chem. Phys.* **2008**, *10*, 3345. (d) Russ, N. J.; Crawford, T. D. *Chem. Phys. Lett.* **2004**, *400*, 104.
(45) (a) Li, S.; Ma, J.; Jiang, Y. *J. Comput. Chem.* **2002**, *23*, 237. (b) Li, S.; Shen, J.; Li, W.; Jiang, Y. *J. Chem. Phys.* **2006**, *125*, 074109.
(46) Li, W.; Gour, J. R.; Piecuch, P.; Li, S. *J. Chem. Phys.* **2009**, *131*, 114109.
(47) Li, W.; Piecuch, P. *J. Phys. Chem. A* **2010**, *114*, 8644.
(48) Li, W.; Piecuch, P. *J. Phys. Chem. A* **2010**, *114*, 6721.
(49) Arora, P.; Li, W.; Piecuch, P.; Evans, J. W.; Albao, M.; Gordon, M. S. *J. Phys. Chem. C* **2010**, *114*, 12649.
(50) (a) Flocke, N.; Bartlett, R. J. *J. Chem. Phys.* **2004**, *121*, 10935. (b) Hughes, T. F.; Flocke, N.; Bartlett, R. J. *J. Phys. Chem. A* **2008**, *112*, 5994. (c) Li, Q.; Yi, Y.; Shuai, Z. *J. Comput. Chem.* **2008**, *29*, 1650.
(51) Auer, A. A.; Nooijen, M. *J. Chem. Phys.* **2006**, *125*, 024104.
(52) Christiansen, O.; Manninen, P.; Jørgensen, P.; Olsen, J. *J. Chem. Phys.* **2006**, *124*, 084103.
(53) (a) Kobayashi, M.; Nakai, H. *J. Chem. Phys.* **2008**, *129*, 044103. (b) Kobayashi, M.; Nakai, H. *J. Chem. Phys.* **2009**, *131*, 114108.
(54) Neese, F.; Hansen, A.; Liakos, D. G. *J. Chem. Phys.* **2009**, *131*, 064103.
(55) (a) Walter, D.; Szilva, A. B.; Niedelfeldt, K.; Carter, E. A. *J. Chem. Phys.* **2002**, *117*, 1982. (b) Walter, D.; Carter, E. A. *Chem. Phys. Lett.* **2001**, *346*, 177. (c) Walter, D.; Venkatnathan, A.; Carter, E. A. *J. Chem. Phys.* **2003**, *118*, 8127. (d) Chwee, T. S.; Szilva, A. B.; Lindh, R.; Carter, E. A. *J. Chem. Phys.* **2008**, *128*, 224106.
(56) (a) Kitaura, K.; Ikeo, E.; Asada, T.; Nakano, T.; Uebayasi, M. *Chem. Phys. Lett.* **1999**, *313*, 701. (b) Kitaura, K.; Sugiki, S.-I.; Nakano, T.; Komeiji, Y.; Uebayasi, M. *Chem. Phys. Lett.* **2001**, *336*, 163.
(57) Fedorov, D. G.; Kitaura, K. *J. Chem. Phys.* **2005**, *123*, 134103.
(58) (a) Li, W.; Li, S. *J. Chem. Phys.* **2004**, *121*, 6649. (b) Netzloff, H. M.; Collins, M. A. *J. Chem. Phys.* **2007**, *127*, 134113.
(59) (a) Stoll, H. *J. Chem. Phys.* **1992**, *97*, 8449. (b) Paulus, B. *Int. J. Quantum Chem.* **2004**, *100*, 1026. (c) Friedrich, J.; Dolg, M. *J. Chem. Theory Comput.* **2009**, *5*, 287.
(60) Gordon, M. S.; Mullin, J. M.; Pruitt, S. R.; Roskop, L. B.; Slipchenko, L. V.; Boatz, J. A. *J. Phys. Chem. B* **2009**, *113*, 9646 and references therein.
(61) (a) Rendell, A. P.; Lee, T. J.; Komornicki, A. *Chem. Phys. Lett.* **1991**, *178*, 462. (b) Rendell, A. P.; Lee, T. J.; Lindh, R. *Chem. Phys. Lett.* **1992**, *194*, 84. (c) Rendell, A. P.; Guest, M. F.; Kendall, R. A. *J. Comput. Chem.* **1993**, *14*, 1429. (d) Kobayashi, R.; Rendell, A. P. *Chem. Phys. Lett.* **1997**, *265*, 1. (e) Piecuch, P.; Landman, J. I. *Parallel Comp.* **2000**, *26*, 913. (f) Hirata, S. *J. Phys. Chem. A* **2003**, *107*, 9887. (g) Baumgartner, G.; Auer, A.; Bernholdt, D. E.; Bibireata, A.; Choppella, V.; Cociorva, D.; Gao, X.; Harrison, R. J.; Hirata, S.; Krishnamoorthy, S.; Krishnan, S.; Lam, C.; Lu, Q.; Nooijen, M.; Pitzer, R. M.; Ramanujam, J.; Sadayappan, P.; Sibiryakov, A. *Proc. IEEE* **2005**, *93*, 276. (h) Piecuch, P.; Hirata, S.; Kowalski, K.; Fan, P.-D.; Windus, T. L. *Int. J. Quantum Chem.* **2006**, *106*, 79. (i) Janowski, T.; Ford, A. R.; Pulay, P. *J. Chem. Theory Comput.* **2007**, *3*, 1368. (j) Harding, M. E.; Metzroth, T.; Gauss, J.; Auer, A. A. *J. Chem. Theory Comput.* **2008**, *4*, 64. (k) Lotrich, V.; Flocke, N.; Ponton, M.; Yau, A. D.; Perera, A.; Deumens, E.; Bartlett, R. J. *J. Chem. Phys.* **2008**, *128*, 194104. (l) Fan, P.-D.; Valiev, M.; Kowalski, K. *Chem. Phys. Lett.* **2008**, *458*, 205. (m) Kowalski, K.; Hammond, J. R.; de Jong, W. A.; Sadlej, A. J. *J. Chem. Phys.* **2008**, *129*, 226101. (n) Aprà, E.; Rendell, A. P.; Harrison, R. J.; Tipparaju, V.; de Jong, W. A.; Xantheas, S. S. In *Proceedings of the Conference on High Performance Computing Networking, Storage and Analysis*; ACM: New York, 2009; ISBN:978-1-60558-744-8, article no. 66 (7 pages). (o) Kuś, T.; Lotrich, V. F.; Bartlett, R. J. *J. Chem. Phys.* **2009**, *130*, 124122. (p) Prochnow, E.; Harding, M. E.; Gauss, J. *J. Chem. Theory Comput.* **2010**, *6*, 2339. (q) Brabec, J.; Krishnamoorthy, S.; Van Dam, H. J. J.; Kowalski, K.; Pittner, J. *Chem. Phys. Lett.* **2011**, *514*, 347. (r) Brabec, J.; Pittner, J.; Van Dam, H. J. J.; Aprà, E.; Kowalski, K. *J. Chem. Theory Comput.* **2012**, *8*, 487.
(62) (a) Olson, R. M.; Bentz, J. L.; Kendall, R. A.; Schmidt, M. W.; Gordon, M. S. *J. Chem. Theory Comput.* **2007**, *3*, 1312. (b) Bentz, J. L.; Olson, R. M.; Gordon, M. S.; Schmidt, M. W.; Kendall, R. A. *Comput. Phys. Commun.* **2007**, *176*, 589.
(63) Andruniow, T.; Zgierski, M. Z.; Kozlowski, P. M. *J. Am. Chem. Soc.* **2001**, *123*, 2679.
(64) Dölker, N.; Maseras, F.; Lledos, A. *J. Phys. Chem. B.* **2003**, *107*, 306.
(65) Kozlowski, P. M.; Zgierski, M. Z. *J. Phys. Chem. B* **2004**, *108*, 14163.

(66) Dölker, N.; Maseras, F.; Siegbahn, P. E. M. *Chem. Phys. Lett.* **2004**, *386*, 174.
(67) Dölker, N.; Morreale, A.; Maseras, F. *J. Biol. Inorg. Chem.* **2005**, *10*, 509.
(68) Becke, A. D. *J. Chem. Phys.* **1993**, *98*, 5648.
(69) Lee, C.; Yang, W.; Parr, R. G. *Phys. Rev. B* **1988**, *37*, 785.
(70) Siegbahn, P. E. M; Borowski, T. *Acc. Chem. Res.* **2006**, *39*, 729 and references therein.
(71) Jensen, K. P.; Ryde, U. *J. Phys. Chem. A* **2003**, *107*, 7539.
(72) (a) Becke, A. D. *J. Chem. Phys.* **1986**, *84*, 4524. (b) Perdew, J. P. *Phys. Rev. B* **1986**, *33*, 8822.
(73) Kuta, J.; Patchkovskii, S.; Zgierski, M. Z.; Kozlowski, P. M. *J. Comput. Chem.* **2006**, *27*, 1429.
(74) (a) Rovira, C.; Biarnes, X.; Kunc, K. *Inorg. Chem.* **2004**, *43*, 6628. (b) Rovira, C.; Kozlowski, P. M. *J. Phys. Chem. B* **2007**, *111*, 3251.
(75) Jensen, K. P.; Ryde, U. *J. Am. Chem. Soc.* **2005**, *127*, 9117.
(76) (a) Kwiecien, R. A.; Khavrutskii, I. V.; Musaev, D. G.; Morokuma, K.; Banerjee, R.; Paneth, P. *J. Am. Chem. Soc.* **2006**, *128*, 1287. (b) Li, X.; Chung, L. W.; Paneth, P.; Morokuma, K. *J. Am. Chem. Soc.* **2009**, *131*, 5115.
(77) (a) Jaworska, M.; Lodowski, P.; Andruniow, T.; Kozlowski, P. M. *J. Phys. Chem. B* **2007**, *111*, 2419. (b) Lodowski, P.; Jaworska, M.; Andruniow, T.; Kozlowski, P. M. *J. Phys. Chem. B* **2009**, *113*, 6898.
(78) Kozlowski, P. M.; Kamachi, T.; Toraya, T.; Yoshizawa, K. *Angew. Chem., Int. Ed.* **2007**, *46*, 980.
(79) (a) Kozlowski, P. M.; Kuta, J.; Galezowski, W. *J. Phys. Chem. B* **2007**, *111*, 7638. (b) Galezowski, W.; Kuta, J.; Kozlowski, P. M. *J. Phys. Chem. B* **2008**, *112*, 3177.
(80) (a) Kumar, M.; Kozlowski, P. M. *J. Phys. Chem. B* **2009**, *113*, 9050. (b) Kozlowski, P. M.; Kamachi, T.; Kumar, M.; Nakayama, T.; Yoshizawa, K. *J. Phys. Chem. B* **2010**, *114*, 5928.
(81) Kuta, J.; Wuerges, J.; Randaccio, L.; Kozlowski, P. M. *J. Phys. Chem. A* **2009**, *113*, 11604.
(82) Jensen, K.; Ryde, U. *Coor. Chem. Rev.* **2009**, *253*, 769.
(83) (a) Solheim, H.; Kornobis, K.; Ruud, K.; Kozlowski, P. M. *J. Phys. Chem. B* **2011**, *115*, 737. (b) Kornobis, K.; Kumar, N.; Wong, B. M.; Lodowski, P.; Jaworska, M.; Andruniow, T.; Ruud, K.; Kozlowski, P. M. *J. Phys. Chem. A* **2011**, *115*, 1280.
(84) Cramer, C. J.; Włoch, M.; Piecuch, P.; Puzzarini, C.; Gagliardi, L. *J. Phys. Chem. A* **2006**, *110*, 1991; **2007**, *111*, 4871 [Addition/Correction].
(85) Rode, M. F.; Werner, H.-J. *Theor. Chem. Acc.* **2005**, *114*, 309.
(86) (a) Kowalski, K.; Piecuch, P. *J. Chem. Phys.* **2000**, *113*, 18. (b) Piecuch, P.; Kowalski, K. In *Computational Chemistry: Reviews of Current Trends*; Leszczyński, J., Ed.; World Scientific: Singapore, 2000; Vol. *5*, pp 1−105.
(87) (a) Piecuch, P.; Kowalski, K.; Pimienta, I. S. O.; McGuire, M. J. *Int. Rev. Phys. Chem.* **2002**, *21*, 527. (b) Piecuch, P.; Kowalski, K.; Pimienta, I. S. O.; Fan, P.-D.; Lodriguito, M.; McGuire, M. J.; Kucharski, S. A.; Kuś, T.; Musiał, M. *Theor. Chem. Acc.* **2004**, *112*, 349.
(88) (a) Piecuch, P.; Włoch, M. *J. Chem. Phys.* **2005**, *123*, 224105. (b) Piecuch, P.; Włoch, M.; Gour, J. R.; Kinal, A. *Chem. Phys. Lett.* **2006**, *418*, 467. (c) Włoch, M.; Gour, J. R.; Piecuch, P. *J. Phys. Chem. A* **2007**, *111*, 11359.
(89) (a) Kinal, A.; Piecuch, P. *J. Phys. Chem. A* **2007**, *111*, 734. (b) Piecuch, P.; Włoch, M.; Varandas, A. J. C. *Theor. Chem. Acc.* **2008**, *120*, 59. (c) Song, Y. Z.; Kinal, A.; Caridade, P. J. S. B.; Varandas, A. J. C.; Piecuch, P. *THEOCHEM* **2008**, *859*, 22. (d) Ge, Y.; Gordon, M. S.; Piecuch, P. *J. Chem. Phys.* **2007**, *127*, 174106. (e) Ge, Y.; Gordon, M. S.; Piecuch, P.; Włoch, M.; Gour, J. R. *J. Phys. Chem. A* **2008**, *112*, 11873. (f) Zheng, J.; Gour, J. R.; Lutz, J. J.; Włoch, M.; Piecuch, P.; Truhlar, D. G. *J. Chem. Phys.* **2008**, *128*, 044108. (g) Zhao, Y.; Tishchenko, O.; Gour, J. R.; Li, W.; Lutz, J. J.; Piecuch, P.; Truhlar, D. G. *J. Phys. Chem. A* **2009**, *113*, 5786. (h) Magoon, G. R.; Aguilera-Iparraguirre, J.; Green, W. H.; Lutz, J. J.; Piecuch, P.; Oluwole, O. O.; Won, H.-W. *Int. J. Chem. Kinet.* **2012**, *44*, 179. (i) Nedd, S. A.; De Yonker, N. J.; Wilson, A. K.; Piecuch, P.; Gordon, M. S. *J. Chem. Phys.* **2012**, *136*, 144109.
(90) (a) Cramer, C. J.; Kinal, A.; Włoch, M.; Piecuch, P.; Gagliardi, L. *J. Phys. Chem. A* **2006**, *110*, 11557; **2007**, *111*, 4871 [Addition/Correction]. (b) Cramer, C. J.; Gour, J. R.; Kinal, A.; Włoch, M.; Piecuch, P.; Shahi, A. R. M.; Gagliardi, L. *J. Phys. Chem. A* **2008**, *112*, 3754.
(91) Raghavachari, K.; Trucks, G. W.; Pople, J. A.; Head-Gordon, M. *Chem. Phys. Lett.* **1989**, *157*, 479.
(92) Roos, B. O. In *Ab Initio Methods in Quantum Chemistry*; Lawley, K. P., Ed.; Wiley: New York, 1987; Vol. *2*, pp 399−445.
(93) Andersson, K.; Malmqvist, P.-Å.; Roos, B. O.; Sadlej, A. J.; Wolinski, K. *J. Phys. Chem.* **1990**, *94*, 5483.
(94) Siegbahn, P. E. M.; Bloomberg, M. R. A.; Chen, S.-L. *J. Chem. Theory Comput.* **2010**, *6*, 2040.
(95) Chen, S.-L.; Bloomberg, M. R. A.; Siegbahn, P. E. M. *J. Phys. Chem. B* **2011**, *115*, 4066.
(96) Reiher, M.; Salomon, O.; Hess, B. A. *Theor. Chem. Acc.* **2001**, *107*, 48.
(97) Ryde, U.; Mata, R. A.; Grimme, S. *Dalton Trans.* **2011**, *40*, 11176.
(98) Hirao, H. *J. Phys. Chem. A* **2011**, *115*, 9308.
(99) Wu, Q.; Yang, W. *J. Chem. Phys.* **2002**, *116*, 515.
(100) (a) Grimme, S. *J. Comput. Chem.* **2004**, *25*, 1463. (b) Grimme, S. *J. Comput. Chem.* **2006**, *27*, 1787. (c) Grimme, S.; Antony, J.; Ehrlich, S.; Krieg, H. *J. Chem. Phys.* **2010**, *132*, 154104.
(101) Pernal, K.; Podeszwa, R.; Patkowski, K.; Szalewicz, K. *Phys. Rev. Lett.* **2009**, *103*, 263201.
(102) Rajchel, L.; Zuchowski, P. S.; Szczęśniak, M. M.; Chalasiński, G. *Phys. Rev. Lett.* **2010**, *104*, 163001.
(103) (a) Becke, A. D.; Johnson, E. R. *J. Chem. Phys.* **2005**, *123*, 154101. (b) Becke, A. D.; Johnson, E. R. *J. Chem. Phys.* **2007**, *127*, 154108.
(104) Misquitta, A. J.; Jeziorski, B.; Szalewicz, K. *Phys. Rev. Lett.* **2003**, *91*, 033201.
(105) (a) Chałasiński, G.; Szczęśniak, M. M. *Chem. Rev.* **1994**, *94*, 1723 and references therein. (b) Chałasiński, G.; Szczęśniak, M. M. *Chem. Rev.* **2000**, *100*, 4227 and references therein. (c) Jeziorski, B.; Moszyński, R.; Szalewicz, K. *Chem. Rev.* **1994**, *94*, 1887 and references therein. (d) Piecuch, P. In *Molecules in Physics, Chemistry and Biology*; Maruani, J., Ed.; Kluwer: Dordrecht, The Netherlands, 1988; Vol. *2* Physical Aspects of Molecular Systems, pp 417−505 and references therein. (e) Piecuch, P. *Mol. Phys.* **1986**, *59*, 1067. (f) Piecuch, P. *Mol. Phys.* **1986**, *59*, 1085.
(106) Møller, C.; Plesset, M. S. *Phys. Rev.* **1934**, *46*, 618.
(107) (a) Purvis, G. D., III; Bartlett, R. J. *J. Chem. Phys.* **1982**, *76*, 1910. (b) Cullen, J. M.; Zerner, M. C. *J. Chem. Phys.* **1982**, *77*, 4088.
(108) Kofod, P.; Harris, P.; Larsen, S. *Inorg. Chem.* **1997**, *36*, 2258.
(109) Randaccio, L.; Furlan, M.; Geremia, S.; Slouf, M.; Srnova, I.; Toffoli, D. *Inorg. Chem.* **2000**, *39*, 3403.
(110) Frisch, M. J.; Trucks, G. W.; Schlegel, H. B.; Scuseria, G. E.; Robb, M. A.; Cheeseman, J. R.; Montgomery, J. A., Jr..; Vreven, T.; Kudin, K. N.; Burant, J. C.; Millam, J. M.; Iyengar, S. S.; Tomasi, J.; Barone, V.; Mennucci, B.; Cossi, M.; Scalmani, G.; Rega, N.; Petersson, G. A.; Nakatsuji, H.; Hada, M.; Ehara, M.; Toyota, K.; Fukuda, R.; Hasegawa, J.; Ishida, M.; Nakajima, T.; Honda, Y.; Kitao, O.; Nakai, H.; Klene, M.; Li, X.; Knox, J. E.; Hratchian, H. P.; Cross, J. B.; Bakken, V.; Adamo, C.; Jaramillo, J.; Gomperts, R.; Stratmann, R. E.; Yazyev, O.; Austin, A. J.; Cammi, R.; Pomelli, C.; Ochterski, J. W.; Ayala, P. Y.; Morokuma, K.; Voth, G. A.; Salvador, P.; Dannenberg, J. J.; Zakrzewski, V. G.; Dapprich, S.; Daniels, A. D.; Strain, M. C.; Farkas, O.; Malick, D. K.; Rabuck, A. D.; Raghavachari, K.; Foresman, J. B.; Ortiz, J. V.; Cui, Q.; Baboul, A. G.; Clifford, S.; Cioslowski, J.; Stefanov, B. B.; Liu, G.; Liashenko, A.; Piskorz, P.; Komaromi, I.; Martin, R. L.; Fox, D. J.; Keith, T.; Al-Laham, M. A.; Peng, C. Y.; Nanayakkara, A.; Challacombe, M.; Gill, P. M. W.; Johnson, B.; Chen, W.; Wong, M. W.; Gonzalez, C.; Pople, J. A. *Gaussian 03*, revision C.02; Gaussian, Inc.: Wallingford, CT, 2004.
(111) (a) Hehre, W. J.; Ditchfield, R.; Pople, J. A. *J. Chem. Phys.* **1972**, *56*, 2257. (b) Hariharan, P. C.; Pople, J. A. *Theor. Chim. Acta*

1973, *28*, 213. (c) Rassolov, V.; Pople, J. A.; Ratner, M.; Windus, T. L. *J. Chem. Phys.* **1998**, *109*, 1223.
(112) Fasching, M.; Schmidt, W.; Kräutler, B.; Stupperich, E.; Schmidt, A.; Kratky, C. *Helv. Chim. Acta* **2000**, *80*, 2295.
(113) Tao, J.; Perdew, J. P.; Staroverov, V. N.; Scuseria, G. E. *Phys. Rev. Lett.* **2003**, *91*, 146401.
(114) Becke, A. D. *Phys. Rev. A* **1988**, *38*, 3098.
(115) Handy, N. C.; Cohen, A. *Mol. Phys.* **2001**, *99*, 403.
(116) Adamo, C.; Barone, V. *J. Chem. Phys.* **1998**, *108*, 664.
(117) Becke, A. *J. Chem. Phys.* **1993**, *98*, 1372.
(118) Lynch, B. J.; Zhao, Y.; Truhlar, D. G. *J. Phys. Chem. A* **2003**, *107*, 1384.
(119) Chai, J.-D.; Head-Gordon, M. *Phys. Chem. Chem. Phys.* **2008**, *10*, 6615.
(120) Staroverov, V. N.; Scuseria, G. E.; Tao, J.; Perdew, J. P. *J. Chem. Phys.* **2003**, *119*, 12129.
(121) Lynch, B. J.; Fast, P. L.; Harris, M.; Truhlar, D. G. *J. Phys. Chem. A* **2000**, *104*, 4811.
(122) Zhao, Y.; Truhlar, D. G. *Theor. Chem. Acc.* **2008**, *120*, 215.
(123) Zhao, Y.; Truhlar, D. G. *J. Chem. Phys.* **2006**, *125*, 194101.
(124) (a) Krishnan, R.; Binkley, J. S.; Seeger, R.; Pople, J. A. *J. Chem. Phys.* **1980**, *72*, 650. (b) Clark, T.; Chandrasekhar, J.; Spitznagel, G. W.; Schleyer, P. v. R. *J. Comput. Chem.* **1983**, *4*, 294. (c) Wachters, A. J. *J. Chem. Phys.* **1970**, *52*, 1033. (d) Hay, P. J. *J. Chem. Phys.* **1977**, *66*, 4377. (e) Raghavachari, K.; Trucks, G. W. *J. Chem. Phys.* **1989**, *91*, 1062.
(125) Boys, S. F.; Bernardi, F. *Mol. Phys.* **1970**, *19*, 553.
(126) Schmidt, M. W.; Baldridge, K. K.; Boatz, J. A.; Elbert, S. T.; Gordon, M. S.; Jensen, J. H.; Koseki, S.; Matsunaga, N.; Nguyen, K. A.; Su, S. J.; Windus, T. L.; Dupuis, M.; Montgomery, J. A. *J. Comput. Chem.* **1993**, *14*, 1347.
(127) TURBOMOLE V6.3 2011, a development of University of Karlsruhe and Forschungszentrum Karlsruhe GmbH, 1989−2007, TURBOMOLE GmbH, since 2007; available from http://www.turbomole.com (accessed April 2012).
(128) Piecuch, P.; Kucharski, S. A.; Kowalski, K.; Musiał, M. *Comput. Phys. Commun.* **2002**, *149*, 71.
(129) (a) Svensson, M.; Humbel, S.; Froese, D. J.; Matsubara, T.; Sieber, S.; Morokuma, K. *J. Phys. Chem.* **1996**, *100*, 19357. (b) Humbel, S.; Sieber, S.; Morokuma, K. *J. Chem. Phys.* **1996**, *105*, 1959.
(130) Boys, S. F. *Rev. Mod. Phys.* **1960**, *32*, 296.
(131) Saebø, S.; Tong, W.; Pulay, P. *J. Chem. Phys.* **1993**, *98*, 2170.
(132) (a) Karlström, G.; Lindh, R.; Malmqvist, P.-Å.; Roos, B. O.; Ryde, U.; Veryazov, V.; Widmark, P.-O.; Cossi, M.; Schimmelpfennig, B.; Neogrady, P.; Seijo, L. *Comput. Mater. Sci.* **2003**, *28*, 222. (b) Aquilante, F.; De Vico, L.; Ferré, N.; Ghigo, G.; Malmqvist, P.-Å.; Neogrády, P.; Pedersen, T. B.; Pitonak, M.; Reiher, M.; Roos, B. O.; Serrano-Andrés, L.; Urban, M.; Veryazov, V.; Lindh, R. *J. Comput. Chem.* **2010**, *31*, 224. (c) Code development: Veryazov, V.; Widmark, P.-O.; Serrano-Andres, L.; Lindh, R.; Roos, B. O. *Int. J. Quantum Chem.* **2004**, *100*, 626. (d) The following persons have contributed to the development of MOLCAS: Andersson, K.; Aquilante, F.; Bernhardsson, A.; Blomberg, M. R .A.; Cooper, D. L.; Cossi, M.; Devarajan, A.; De Vico, L.; Ferré, N.; Fülscher, M. P.; Gaenko, A.; Gagliardi, L.; Ghigo, G.; de Graaf, C.; Hess, B. A.; Hagberg, D.; Holt, A.; Karlström, G.; Krogh, J. W.; Lindh, R.; Malmqvist, P.-Å.; Neogrády, P.; Olsen, J.; Pedersen, T. B.; Pitonak, M.; Raab, J.; Reiher, M.; Roos, B. O.; Ryde, U.; Schapiro, I.; Schimmelpfennig, B.; Seijo, L.; Serrano-Andrés, L.; Siegbahn, P. E. M.; Stalring, J.; Thorsteinsson, T.; Vancoillie, S.; Veryazov, V.; Widmark, P.-O.; Wolf, A.
(133) Andersson, K.; Roos, B. O. *Chem. Phys. Lett.* **1992**, *191*, 507.
(134) Pierloot, K.; Dumez, B.; Widmark, P.-O.; Roos, B. O. *Theor. Chim. Acta* **1995**, *90*, 87.
(135) Martin, R. L. *J. Phys. Chem.* **1983**, *87*, 750.
(136) Rintelman, J. M.; Adamovic, I.; Varganov, S.; Gordon., M. S. *J. Chem. Phys.* **2005**, *122*, 044105.